

Manuscript Number: JACI-D-17-01273

Title: Autophagic dysfunction in Papillon Lefèvre is restored by  
recombinant Cathepsin C treatment

Article Type: Original Article

Section/Category: Atopic dermatitis and inflammatory skin disease

Keywords: Papillon-Lefèvre; Cathepsin C; autophagy; lysosomal  
permeabilization

Corresponding Author: Dr. Mario D. Cordero, Ph.D

Corresponding Author's Institution: Institute of Nutrition and Food  
Technology "José Mataix Verdú", Department of Physiology, Biomedical  
Research Center, University of Granada

First Author: Pedro Bullón

Order of Authors: Pedro Bullón; Beatriz Castejón-Vega; Lourdes Román-  
Malo; Arturo Falcao; María Paz Jimenez-Guerrero; David Cotán; Tamara Y.  
Forbes-Hernandez; Alfonso Alfonso Varela-López; Francesca Francesca  
Giampieri; José L. Quiles; Maurizio Battino; José A. Sánchez-Alcázar;  
Mario D. Cordero, Ph.D

Manuscript Region of Origin: SPAIN

Abstract: Background: Cathepsin C (CatC) is a lysosomal enzyme involved  
in the degradation of intracellular proteins and associated with the  
autophagic process. Several mutations with loss of function in the  
Cathepsin C (CatC) gene have been shown to be the genetic mark of  
Papillon-Lefèvre syndrome (PLS), a rare autosomal recessive disease  
characterized by severe early-onset periodontitis, palmoplantar  
hyperkeratosis and increased susceptibility to infections. Deficiencies  
or dysfunction in other cathepsins such as B or D have been associated  
with autophagic and lysosomal disorders.

Objectives: Here, we characterized the basis for autophagic dysfunction  
in PLS by analyzing skin fibroblasts from PLS patients with several  
mutations in CatC and reduced enzymatic activity.

Methods: Skin fibroblasts were isolated from patients and characterized  
by genetic study. Autophagy flux was evaluated by accumulation of  
p62/SQSTM1 and bafilomycin assay and confirmed by visible autophagosome  
accumulation by Transmission Electron Microscopy. A recombinant CatC was  
produced by produced by produced by baculovirus system in insect cell  
cultures.

Results: Our data showed metabolic alterations in the  
oxidative/antioxidative status, reduced oxygen consumption and a marked  
autophagic dysfunction with autophagosome accumulation. This was  
associated with lysosomal permeabilization, CatB release and NLRP3-  
inflammasome activation. A treatment with recombinant CatC (rCatC)  
improved cell growth, autophagic flux and partially restored lysosomal  
permeabilization.

Conclusions: Our data provide a novel molecular mechanism of PLS. Dysfunctional autophagy as a secondary event resulting from insufficient lysosomal function in PLS could show a new therapeutic target.

## Journal of Allergy and Clinical Immunology Manuscript Review

*In order to be eligible to receive CME credit for your review, you must read the following information.*

### ***Educational Learning Objectives***

1. To update knowledge of the current literature through literature searches conducted for critique of manuscripts
2. To glean new information and understanding of specific areas of study that can impact the reviewers' research or practice
3. To exercise and expand use of critical analytical skills
4. To develop teaching skills by advising authors on study design, scientific method and analysis, and scientific writing
5. To contribute to expansion of the body of knowledge in allergy/ immunology

### ***Accreditation Statement***

This activity has been planned and implemented in accordance with the Essential Areas and Policies of the Accreditation Council for Continuing Medical Education (ACCME) by the American Academy of Allergy, Asthma and Immunology (AAAAI). The AAAAI is accredited by the ACCME to provide continuing medical education for physicians.

### ***Designation Statement***

The American Academy of Allergy, Asthma and Immunology designates this educational activity for 3.0 *AMA PRA Category 1 Credits*<sup>™</sup> per review, with a maximum of 15.0 credits per calendar year. Physicians should only claim credit commensurate with the extent of their participation in the activity.

### ***Target Audience***

This activity is intended for board-certified physicians and researchers in the fields of allergy and immunology.

### ***Overall Purpose/Goal***

The purpose of this activity is to affirm or modify knowledge, competence, or performance as a result of reading the manuscript.

### **DESIGN COMMITTEE:**

**Cezmi Akdis, MD FAAAAI (Co-Editor-in-Chief); Employer:** Swiss Institute of Allergy and Asthma Research B) University of Zurich, Switzerland Title: A) Director (SIAF) B) Medical Faculty (University of Zurich) **Competing Relationships:** Advisory Board: Circassia (United Kingdom), Allergopharma (Germany), Novartis (Basel, Switzerland), Teva (Amsterdam, the Netherlands), Anergis (Lausanne, Switzerland); Shareholder (Ongoing): Alimentary Health Pharma (Davos, Switzerland); Shareholder (Ongoing): Davos Diagnostics (Davos, Switzerland) **Organizational Interests:** CK-CARE Christine Kühne - Center for Allergy Research and Education (Ongoing); Directorium Member; GA2LEN, Global Allergy And Asthma European

Network (Ongoing): Ex-com Member World Immune Regulation Meetings (Ongoing): Chair, Organizer.

**Andrea Apter, MD MA MSc FAAAAI: Employer:** University of Pennsylvania (Professor of Medicine) **Competing Relationships:** NHLBI: RC1 (funded-now complete) - PI, NHLBI (Ongoing): R18, PCORI (Ongoing): PI. **Organizational Interests:** American College of Asthma Allergy & Immunology (Ongoing): Fellow, American College of Physicians (Ongoing): Fellow, American Thoracic Society (Ongoing): Behavioral Science Assembly program committee, Associate Editor (Ongoing): Journal of Allergy & Clinical Immunology, Consultant (Ongoing): UPTODATE. **Conflict Resolution:** The research grant from Bristol-Myers Squibb and AstraZeneca is paid directly to my institution, and 2.5% of my salary is supported by these grant funds. The research focuses on a diabetes drug, and is not related to any of their respiratory products.

**Leonard Bacharier, MD FAAAAI: Employer:** Washington University (Professor of Pediatrics) **Competing Relationships:** AstraZeneca China (Ongoing): Honoraria for lectures, DBV Technologies (Ongoing): Consultant, Novartis (Ongoing): Honoraria for lectures, Teva (Ongoing): Honoraria for lectures, consultant, Sanofi (Ongoing): Advisory Board attendance, NIH/NHLBI/NIAID (Ongoing): Investigator: AsthmaNet, Severe Asthma Research Program, Inner City Asthma Consortium. **Organizational Interests:** AAAAI (Ongoing): Fellow, Editorial Boards of JACI and JACI: In practice, AMPC Member (Ongoing). **Conflict Resolution:** Will present data from a variety of published peer-reviewed studies.

**Claus Bachert, MD PhD: Employer:** Universitair Ziekenhuis Gent (Professor, Chief of Clinics) **Competing Relationships:** ALK (Ongoing): speaker, Allergopharma: speaker, board, Bionorica (Ongoing): speaker, board, Genentech: board, Meda (Ongoing): speaker, board, MSD (Ongoing): speaker, Novartis (Ongoing): board, Stallergenes (Ongoing): speaker, Uriach (Ongoing): speaker, board. **Organizational Interests:** DGAKI (Ongoing): Vice President, WAO (Ongoing): Executive Board. **Conflict Resolution:** Spread of bias over many companies, no direct influence in any presentations.

**Zuhair K. Ballas, MD FAAAAI: Employer:** University of Iowa Health Care (Professor of Medicine) **Competing Relationships:** Honorarium/Gift: Up-To-Date, Immune Deficiency Foundation, NIH (Ongoing): Received grant, Veterans Administration (Ongoing): Received Merit grant. **Organizational Interests:** Clinical Immunology Society (Ongoing): Member of Nominating committee, Immune Deficiency Foundation (Ongoing): immunodeficiency consultant, Medical Advisory Council.

**Joshua A. Boyce, MD FAAAAI: Employer:** Brigham and Women's Hospital (Albert L. Sheffer Prof of Medicine; Director, Inflammation and Allergic Disease Research Section) **Organizational Interests:** Consultant: Calcimedica, LPath, Inc. (Ongoing).

**Robert K. Bush, MD FAAAAI: Employer:** Retired; **Competing Relationships:** Honorarium/Gift: Section editor Current Opinion in Allergy&Clinical Immunology and Current Allergy Reports, Honorarium/Gift: Section editor Allergy & Immunology Reports

**Javier Chinen, MD PhD FAAAAI: Employer:** Baylor College of Medicine (Associate Professor) **Nothing to disclose.**

**Raif S. Geha, MD FAAAAI: Employer:** Children's Hospital of Boston (Chief, Div. Imm., Prof. Ped.) **Nothing to disclose.**

**Kenji Kabashima, MD PhD: Employer:** Kyoto University (Professor) **Competing Relationships:** A\*Star (Senior Principal Investigator) **Competing Relationships: Advisory Board:** Chugai, Janssen, Ono Pharmaceutical (Ongoing), Daiichi Sankyo, Polo Pharma, Kao Co.

**Carole Ober, PhD: Employer:** University of Chicago (Professor) **Nothing to disclose.**

**David B. Peden, MD MS FAAAAI: Employer:** University NC School Medicine (Andrews Distinguished Professor of Pediatrics, Medicine and Microbiology/Immunology) **Nothing to disclose.**

**Harald E. Renz, MD FAAAAI: Employer:** Philipps University Marburg (Professor and Director) **Organizational Interests:** Deutsche Gesellschaft für Klinische Chemie und Laboratoriumsmedizin (DGKL) (Ongoing): Chairman Working Group Autoimmune Diagnostics Deutsche Gesellschaft für Allergologie und Klinische Immunologie (DGAKI) (Ongoing): President.

**Marc E. Rothenberg, MD PhD FAAAAI: Employer:** Cincinnati Children's Hospital Medical Center (Director of the Division of Allergy and Immunology) **Competing Relationships:** Consultant: Novartis, NKT Therapeutics, Celsus Pharmaceuticals (Ongoing), Immune Pharmaceuticals (Ongoing), Receptos. **Organizational Interests:** American Partnership for Eosinophilic Disorders (Ongoing): Member, Medical Advisory Board CEGIR (Consortium of Eosinophilic Gastrointestinal Disease Researchers) (Ongoing): Principal Investigator, International Eosinophil Society (Ongoing): Steering Committee TIGERS (Ongoing): Steering Committee. **Conflict Resolution:** I present unbiased information in my activities for the AAAAI, and I am not currently studying any product produced by these companies.

**Hirohisa Saito, MD PhD FAAAAI: Employer:** National Research Institute for Child Health & Development (Deputy Director of the Research Institute) **Competing Relationships:** Speaker: Teijin Pharma Ltd, Shiseido Co.,Ltd., MSD (Merck Sharp and Dohme) K.K., Ono Pharmaceutical Co., Ltd., GlaxoSmithKline K.K., Pfizer Japan Inc., Kyowa Hakko Kirin, Kyorin Pharmaceutical, Daiichi Sankyo.

**Stanley Szeffler, MD FAAAAI: Employer:** University of Colorado Denver School of Medicine (Professor of Pediatrics; Head, Pediatric Asthma Research) **Competing Relationships:** Advisory Board: Aerocrine, Boehringer-Ingelheim, Novartis, Roche, Glaxo Smith Kline. NIH:NHLBI (Ongoing): Research Grant: AsthmaNet, NIH:NIEHS/EPA (Ongoing): Research Grant: Childhood Health and Environmental Center Grant, Colorado Public Health Department (Ongoing): Research Grant, NIH:NIAID (Ongoing): Research Grant: Inner City Asthma Consortium. **Organizational Interests:** AAAAI (Ongoing): Fellow; Deputy Editor For Journal

of Allergy and Clinical Immunology, ACAAI (Ongoing): Fellow, American Academy of Pediatrics (Ongoing): Fellow, American Thoracic Society (Ongoing): Member, Colorado Allergy and Asthma Society (Ongoing): Member. **Conflict Resolution:** I disclose my potential conflicts at all meetings and lectures. I focus my working relationships on research and providing advice on drug development, as well as overseeing research studies. I do not provide lectures that serve as marketing formats for specific drugs. I also disclose all of my financial relationships to University of Colorado for ongoing review.

**Stephan Weidinger, MD, PhD**

**Employer:** Christian-Albrechts-University of Kiel and University Hospital Schleswig-Holstein.

**Competing Relationships:** Speaker: Sanofi-Aventis, Novartis, Galderma. Advisory Boards: Astellas, Novartis, Sanofi-Aventis. Research Grants: Sanofi-Aventis (ongoing), La Roche Posay (ongoing), Novartis (finished), Pfizer (finished), Biogen (finished).

Organizational Interests: EAACI (secretary dermatology section); Associate Editor for Journal of Investigative Dermatology, Allergy

**Robert A. Wood, MD FAAAAI: Employer:** Johns Hopkins University School Medicine (Professor of Pediatrics) **Competing Relationships:** Research Grants: NIAID (Ongoing), DBV Technologies (Ongoing), Aimmune (Ongoing), Astellas (Ongoing) Up To Date (Ongoing): Royalties.

**FACULTY DISCLOSURES**

Please refer to the opening pages of the assigned manuscript for the authors' relevant funding and employment information.



Cezmi A. Akdis, Editor-in-Chief  
Journal of Allergy and Clinical Immunology

September 06, 2017

Dear Editor,

We would like to submit our manuscript: "**Autophagic dysfunction in Papillon Lefèvre is restored by recombinant Cathepsin C treatment**" to be considered for publication in *Trends in Immunology*, in form of an original contribution.

Papillon-Lefèvre syndrome (PLS) is a rare autosomal recessive condition characterized by severe early-onset periodontitis and palmoplantar hyperkeratosis and where dermatological symptoms begin prior to 2 years of age and continue throughout life 2 accompanied by increased susceptibility to infections, furunculosis and pyoderma, or pyogenic liver abscess, among others. PLS results from mutations that inactivate or introduce loss of function in the Cathepsin C (CatC) gene.

In this study, we have described for first time the implication of the autophagic dysfunction and lysosomal permeabilization in the pathophysiology of skin fibroblasts from PLS. Furthermore, we show a partial reconstitution of the pathological process after treatment with a recombinant CatC produced by produced by baculovirus system in insect cell cultures.

In summary, we believe that our study considerably enriches the perception of pathogenic mechanisms of the dermatological alterations of PLS and propose new pharmacological targets.

I hereby state:

1. That the submitting author has the written consent from all authors to submit the manuscript and that all authors accept complete responsibility for the contents of the manuscript
2. That the manuscript is not currently under consideration elsewhere and the work reported will not be submitted for publication elsewhere until a final decision has been made as to its acceptability by the Journal
3. That the manuscript is truthful original work

Yours sincerely

Dr. Mario D. Cordero  
Institute of Nutrition and Food Technology "José Mataix Verdú", Department of  
Physiology, Biomedical Research Center, University of Granada, 18100 Granada, Spain.  
+34-958-241-000 (ext. 20316), Email: [mdcormor@us.es](mailto:mdcormor@us.es).

1 **Autophagic dysfunction in Papillon Lefèvre is restored by recombinant Cathepsin**  
2 **C treatment**

3 Pedro Bullón, MD, PhD<sup>1,2\*</sup>, Beatriz Castejón-Vega, BSc<sup>1\*</sup>, Lourdes Román-Malo,  
4 PhD<sup>1,2</sup>, Arturo Falcao, BSc<sup>1</sup>, María Paz Jimenez-Guerrero, BSc<sup>3</sup>, David Cotán, PhD<sup>3</sup>,  
5 Tamara Y. Forbes-Hernandez, PhD<sup>4</sup>, Alfonso Varela-López, PhD<sup>5</sup>, Antonio Pérez-  
6 Pulido, PhD<sup>6</sup>, Francesca Giampieri, PhD<sup>4</sup>, José L. Quiles, PhD<sup>5</sup>, Maurizio Battino,  
7 PhD<sup>4</sup>, José A. Sánchez-Alcázar, MD, PhD<sup>3</sup>, Mario D. Cordero, PhD<sup>5,7</sup>

8 <sup>1</sup> Research Laboratory, Dental School, University of Sevilla, Sevilla, Spain

9 <sup>2</sup> Dept. of Periodontology, Dental School, University of Sevilla, Spain.

10 <sup>3</sup> Centro Andaluz de Biología del Desarrollo (CABD), Consejo Superior de  
11 Investigaciones Científicas, Universidad Pablo de Olavide, Carretera de Utrera Km 1,  
12 Sevilla, 41013, Spain

13 <sup>4</sup> Dipartimento di Scienze Cliniche Specialistiche ed Odontostomatologiche, Sez.  
14 Biochimica, Università Politecnica delle Marche, 60131, Ancona, Italy.

15 <sup>5</sup> Department of Physiology, Institute of Nutrition and Food Technology "José Mataix",  
16 Biomedical Research Center (CIBM), University of Granada, Armilla, Avda. del  
17 Conocimiento s.n., 18100 Armilla, Spain.

18 <sup>6</sup> Centro Andaluz de Biología del Desarrollo (CABD), Universidad Pablo de Olavide-  
19 CSIC-Junta de Andalucía.

20 <sup>7</sup> Senior author of the study

21 \* These authors contributed equally to this work.

22 **Running Title:** Autophagic dysfunction in Papillon Lefèvre

23

24 **Corresponding Author:**

25 Dr. Mario D. Cordero (Senior)

26 Institute of Nutrition and Food Technology "José Mataix Verdú", Department of  
27 Physiology, Biomedical Research Center, University of Granada, 18100 Granada,  
28 Spain. +34-958-241-000 (ext. 20316), Email: [mdcormor@ugr.es](mailto:mdcormor@ugr.es)



29 Dr. Maurizio Battino

30 Dipartimento di Scienze Cliniche Specialistiche ed Odontostomatologiche – Sez

31 Biochimica. Università Politecnica delle Marche

32 Via Ranieri, 65. 60100 Ancona, Italy, Email: [m.a.battino@univpm.it](mailto:m.a.battino@univpm.it)

33

34

35

36 **Abstract**

37 **Background:** Cathepsin C (CatC) is a lysosomal enzyme involved in the degradation of  
38 intracellular proteins and associated with the autophagic process. Several mutations  
39 with loss of function in the Cathepsin C (CatC) gene have been shown to be the genetic  
40 mark of Papillon-Lefèvre syndrome (PLS), a rare autosomal recessive disease  
41 characterized by severe early-onset periodontitis, palmoplantar hyperkeratosis and  
42 increased susceptibility to infections. Deficiencies or dysfunction in other cathepsins  
43 such as B or D have been associated with autophagic and lysosomal disorders.

44 **Objectives:** Here, we characterized the basis for autophagic dysfunction in PLS by  
45 analyzing skin fibroblasts from PLS patients with several mutations in CatC and  
46 reduced enzymatic activity.

47 **Methods:** Skin fibroblasts were isolated from patients and characterized by genetic  
48 study. Autophagy flux was evaluated by accumulation of p62/SQSTM1 and  
49 bafilomycin assay and confirmed by visible autophagosome accumulation by  
50 Transmission Electron Microscopy. A recombinant CatC was produced by produced by  
51 produced by baculovirus system in insect cell cultures.

52 **Results:** Our data showed metabolic alterations in the oxidative/antioxidative status,  
53 reduced oxygen consumption and a marked autophagic dysfunction with  
54 autophagosome accumulation. This was associated with lysosomal permeabilization,  
55 CatB release and NLRP3-inflammasome activation. A treatment with recombinant CatC  
56 (rCatC) improved cell growth, autophagic flux and partially restored lysosomal  
57 permeabilization.

58 **Conclusions:** Our data provide a novel molecular mechanism of PLS. Dysfunctional  
59 autophagy as a secondary event resulting from insufficient lysosomal function in PLS  
60 could show a new therapeutic target.

61 **Keywords:** Papillon-Lefèvre, Cathepsin C, autophagy, lysosomal permeabilization

62

## 63 **Introduction**

64 Papillon-Lefèvre syndrome (PLS) is a rare autosomal recessive condition characterized  
65 by severe early-onset periodontitis and palmoplantar hyperkeratosis resulting in a  
66 premature loss of both deciduous and permanent dentitions <sup>1</sup>. Dermatological symptoms  
67 in PLS begin prior to 2 years of age and continue throughout life <sup>2</sup>. About 20–25% of  
68 PLS patients report an increased susceptibility to infections, such as furunculosis and  
69 pyoderma, or pyogenic liver abscess, among others <sup>2</sup>. PLS results from mutations that  
70 inactivate or introduce loss of function in the Cathepsin C (CatC) gene, which is  
71 associated with lack of immune cell serine protease activities <sup>3</sup>, hyperactive neutrophils  
72 <sup>4</sup>, increased oxidative stress <sup>2</sup> and decreased neutrophil extracellular traps capacity as a  
73 defensive form against microorganisms <sup>5</sup>.

74 CatC is a lysosomal enzyme involved in the degradation of intracellular proteins <sup>6</sup>. This  
75 process is mediated by autophagy, a critical mechanism devoted to preserving cellular  
76 homeostasis. The cellular turnover of proteins and organelles requires the cooperation  
77 between autophagic and lysosomal degradation pathways where the fusion of the  
78 autophagosome with the lysosome has a relevant role <sup>7</sup>. As a pathological process, it is  
79 known that accumulation of undegraded substrates in lysosomes, due to a deficiency of  
80 lysosomal enzymes, impairs the fusion between autophagosomes and lysosomes. This is  
81 the molecular base of a set of pathological conditions, known as lysosomal storage  
82 diseases like Gaucher disease or Niemann pick disease <sup>8</sup>.

83 To date, the autophagy pathway has never been studied in PLS. However, reduced  
84 activity of CatC could induce accumulation of undegraded substrates dysfunctional  
85 organelles. In the present study, we show an autophagic dysfunction in fibroblasts from  
86 PLS patients with accumulation of p62/SQSTM1 and visible autophagosome

87 accumulation by TEM (Transmission Electron Microscopy) proposing an impaired  
88 autophagic flux, which was confirmed by bafilomycin assay. An important increment of  
89 another cathepsin enzyme, cathepsin B (CatB), was observed and associated with  
90 lysosomal permeabilization. Treatment with recombinant CatC in the fibroblasts from  
91 PLS patients showed a partial recovery.

## 92 **MATERIAL AND METHODS**

### 93 **Ethical Statements**

94 Approval of the ethical committee of the University of Seville was obtained, according  
95 to the principles of the Declaration of Helsinki and all the International Conferences on  
96 Harmonization and Good Clinical Practice Guidelines. All the participants in the study  
97 gave their written informed consent before initiating it.

### 98 **Reagents.**

99 Trypsin and bafilomycin A1 were purchased from Sigma Chemical Co., (St. Louis,  
100 Missouri). Anti-GAPDH monoclonal antibody from Calbiochem-Merck Chemicals Ltd.  
101 (Nottingham, UK). Anti-NLRP3 antibody from Adipogen (San Diego, USA) from  
102 Santa Cruz Biotechnology. Anti-active caspase-1, LC3, ATG-12, p62, Lamp-I  
103 Cathepsin B and galectin-3 were obtained from Cell Signaling Technology. A cocktail  
104 of protease inhibitors (complete cocktail) was purchased from Boehringer Mannheim  
105 (Indianapolis, IN). Grace's insect medium was purchased from Gibco. The Immun Star  
106 HRP substrate kit was from Bio-Rad Laboratories Inc. (Hercules, CA).

### 107 **Fibroblast cultures**

108 Patients and control fibroblasts were obtained according to the Helsinki Declarations of  
109 1964, as revised in 2001. Fibroblasts were cultured in high glucose DMEM (Dulbecco's

110 modified media) (Gibco, Invitrogen, Eugene, OR, USA) supplemented with 10% fetal  
111 bovine serum (FBS) (Gibco, Invitrogen, Eugene, OR, USA) and antibiotics (Sigma  
112 Chemical Co., St. Louis, MO, USA). Cells were incubated at 37°C in a 5% CO<sub>2</sub>  
113 atmosphere.

#### 114 **Structure of mutation analysis**

115 The 3D structure of CatC (UniProt:P53634) was obtained from the PDB database using  
116 the identifier 2DJG, which has the native structure of the human cathepsin C at high  
117 resolution and include only a monomer of the molecule. The structure was visualized  
118 with the Rasmol program. The functional annotations of the protein, including the  
119 amino acids corresponding to the active site were obtained from the well-curated  
120 database UniProt.

#### 121 **Enzymatic activity of CatC**

122 CatC activity was determined by measuring the amount of 7-amino-4-methyl coumarin  
123 (NHMeC) released by hydrolysis of a specific substrate (glycyl-L-arginine-7-amido-4-  
124 methylcoumarin, Bachem, UK, www.bachem.com) on incubation with sonicated  
125 peripheral blood leukocytes, as described previously <sup>9</sup>.

#### 126 **Antioxidant enzyme activity**

127 Catalase activity was determined in cellular lysate by monitoring H<sub>2</sub>O<sub>2</sub> decomposition  
128 at 240 nm <sup>10</sup>. SOD activity was determined on the basis of the inhibition of the  
129 formation of NADH–phenazine methosulfate-nitroblue tetrazolium formazan <sup>11</sup>.

#### 130 **Western Blotting for mitochondrial protein**

131 Whole cellular lysate from fibroblasts was prepared by gentle shaking with a buffer  
132 containing 0.9% NaCl, 20 mM Tris-ClH, pH 7.6, 0.1% triton X-100, 1 mM  
133 phenylmethylsulfonylfluoride and 0.01% leupeptine. The protein content was  
134 determined by the Bradford method. Electrophoresis was carried out in a 10–15%

135 acrylamide SDS/PAGE and proteins were transferred to Immobilon membranes  
136 (Amersham Pharmacia, Piscataway, NJ). Next, membranes were washed with PBS,  
137 blocked over night at 4°C and incubated with the respective primary antibody solution  
138 (1:1000). Membranes were then probed with their respective secondary antibody  
139 (1:2500). Immunolabeled proteins were detected using a chemiluminescence method  
140 (Immun Star HRP substrate kit, Bio-Rad Laboratories Inc., Hercules, CA). Western blot  
141 image was quantified using ImageJ software (see:  
142 <http://rsb.info.nih.gov/ij/download.html>).

### 143 **Mitochondrial ROS production**

144 Mitochondrial ROS generation in BMCs and fibroblasts was assessed by MitoSOX™  
145 red, a red mitochondrial superoxide indicator. MitoSOX Red is a novel fluorogenic dye  
146 recently developed and validated for highly selective detection of superoxide in the  
147 mitochondria of live cells. MitoSOX™ Red reagent is live-cell permeant and is rapidly  
148 and selectively targeted to the mitochondria. Once in the mitochondria, MitoSOX™  
149 Red reagent is oxidized by superoxide and exhibits red fluorescence.

150 Flow cytometry. Approximately  $1 \times 10^6$  cells were incubated with  $1 \mu\text{M}$  MitoSOX™ red  
151 for 30 min at 37°C, washed twice with PBS, resuspended in 500  $\mu\text{l}$  of PBS and analyzed  
152 by flow cytometry in an Epics XL cytometer, Beckman Coulter, Brea, California, USA  
153 (excitation at 510 nm and fluorescence detection at 580 nm).

### 154 **Intracellular ROS production**

155 The intracellular ROS levels were determined using the probe CellROX® Orange  
156 reagent (Invitrogen™, Life Technoliges, Milan, Italy) according to the manufacturer's  
157 instructions. Briefly, on the first day of the assay cells were seeded in a 6-well plate at a  
158 density of  $1.5 \times 10^5$  cell/well and allowed to adhere for 16–18 h. The cells were treated

159 with CellROX<sup>®</sup> Orange Reagent which was added to 1 mL of complete medium at a  
160 1:500 (v/v) dilution. Samples were incubated for 30 min at 37 °C, centrifuged at 320 x g  
161 once to remove medium and excess dye, and then resuspended in PBS. After labeling  
162 with CellROX<sup>®</sup> Orange Reagent, cells were analysed with the Tali<sup>®</sup> Image-Based  
163 cytometer (Invitrogen<sup>™</sup>, Life Technologies, Milan, Italy) collecting 20-fields per  
164 sample. Control cells were used to determine baseline levels of intracellular ROS and to  
165 set the fluorescence threshold for the Tali<sup>®</sup> instrument. Each treatment was carried out  
166 in three replicates and the final results were expressed as fold increase compared to  
167 control.

#### 168 **Oxygen consumption rate (OCR)**

169 Oxygen consumption rate (OCR) was assessed in real-time using the Extracellular Flux  
170 Analyzer XF-24 (Seahorse Bioscience, North Billerica, MA, USA) according to the  
171 manufacturer's protocol, which allows to measure OCR changes after injecting up to  
172 four different compounds (stimulators, inhibitors or substrates) affecting bioenergetics.  
173 Cells were seeded at a density of  $5 \times 10^4$  cell/well into the XF-24 cell culture microplate  
174 with the complete growth media and then incubated for 24 h. Before starting  
175 measurements, cells were placed in a running DMEM medium (supplemented with 25  
176 mM glucose, 2 mM glutamine, 1 mM sodium Pyruvate, and without serum) and pre-  
177 incubated for 20 min at 37°C in the absence of CO<sub>2</sub> in the XF Prep Station incubator  
178 (Seahorse Bioscience, Billerica MA, USA). Cells were transferred to the XF-24  
179 Extracellular Flux Analyzer and after an OCR baseline measurement a profiling of  
180 mitochondrial function was performed by sequential injection of the following  
181 compounds : oligomycin (final concentration 2.5 µg/mL) at injection in port A, 2,4-  
182 dinitrophenol (2,4-DNP) (final concentration 1 mM) at injection in port B, and  
183 antimycin/rotenone (final concentration 10 µM/1µM) at injection in port C. A minimum

184 of five wells were utilized per condition in any given experiment. Data are expressed as  
185 pMol of O<sub>2</sub> consumed per minute normalized to 1000 cells (pMol O<sub>2</sub>/1000 cells/min).

### 186 **Electron microscopy**

187 Fibroblasts were fixed for 15 min in the culture plates with 1.5% glutaraldehyde in  
188 culture medium, then for 30 min in 1.5% glutaraldehyde-0.1 M NaCacodylate/HCl, pH  
189 7.4. They were then washed three times in 0.1 M NaCacodylate/HCl, pH 7.4 for 10 min  
190 and post-fixed with 1% OsO<sub>4</sub>-H<sub>2</sub>O, pH 7.4 for 30 min. After dehydration in increasing  
191 concentrations of ethanol, 5 min for each step: 50,70, 90 and three times 100%,  
192 impregnation steps and inclusion were performed in Epon and finally polymerized at  
193 60°C for 48 h. 60–80 nm sections were obtained using an ultramicrotome Leica ultracut  
194 S (Leitz Microsystems, Wetzlar, Germany) and contrasted with uranyl acetate and lead  
195 citrate. Observations were performed on a Zeiss LEO 906 E (Oberkochen, Germany)  
196 transmission electron microscope.

### 197 **Proliferation rate**

198 Two hundred thousand fibroblasts were cultured in the absence or presence of rCatC  
199 (0.25µg) for 24, 48, 72, and 120h. After discharging supernatant with dead cells, cell  
200 counting was performed from 3 high power fields using an inverted microscope and a  
201 40X objective.

### 202 **Cathepsin B release**

203 CatB redistribution from lysosomes/autophagolysosomes to the cytosol was assessed by  
204 immunofluorescence techniques using antibodies against CatB and LAMP-I as a marker  
205 of lysosomal/autophagolysosomal compartment. In control fibroblasts, CatB-specific  
206 immunostainings reveal cytoplasmic puncta structures that are surrounded by



207 lysosomal/autophagolysosomal membrane proteins such as LAMP-I. After lysosomal  
208 permeabilization, the immunofluorescence detection of CatB reveals a diffuse staining  
209 throughout the entire cell.

### 210 **Galectin puncta**

211 Lysosomal permeabilization was also detected by the galectin puncta assay as  
212 previously described <sup>12</sup>.

### 213 **Recombinant Cathepsin C production**

214 Sequence was designed from the literature and an external service (GeneArt Invitrogen)  
215 was used for its synthesis inside a bacterial vector with ampicillin resistance gen.  
216 Construct codifying for recombinant CatC was synthesized and cloned into a pBAC4x  
217 baculovirus transfer vector under the control of the polyhedrin promoter. Sf21 cell line  
218 was co-transfected using a linearized modified *Autographa californica* nuclear  
219 polyhedrosis virus DNA and the created transfer plasmid was transferred by a  
220 lipofectamin-mediated method as specified by the manufacturer (Invitrogen™). The  
221 Sf21 cells were sown in 6 wells-plates (1×10<sup>6</sup> cells/plate). After attachment, the cells  
222 were infected with the recombinant baculovirus at MOI of 5 for 72 h at 27 °C in  
223 darkness. Based on titration of virus obtained by quantitative PCR and the amount of  
224 virus required, the volumes were calculated to infect cells. The infected cells and culture  
225 supernatant were harvested and separated by centrifugation at 800×g for 5min at 4°C.  
226 Cell pellet was homogenized in PBS 1X and protease inhibitor, 1 mM PMSF, then  
227 sonicated with an ultrasonic processor Sonopuls HD2070 (Bandelin) for 3×10 s at 30%  
228 potency. Once the clarified fractions were obtained by centrifugation with recombinant  
229 proteins, these were used in cell cultures assays.

### 230 **Statistical Analysis**

231 Data in the figures is given as mean  $\pm$  SD. Data between different groups were analyzed  
232 statistically by using ANOVA on Ranks with Sigma Plot and Sigma Stat statistical  
233 software (SPSS for Windows, 19, 2010, SPSS Inc. Chicago, IL, USA). For cell-culture  
234 studies, Student's t test was used for data analyses. A value of  $p < 0.05$  was considered  
235 significant.

## 236 **Results**

### 237 **Genetic characterization shows homozygous and heterozygous mutations in CatC** 238 **with clinical phenotype**

239 Three patients were selected for this study. Patient one was a 31-year-old man with  
240 hyperkeratosis in the palmoplantar region and on his hands and moderate periodontitis  
241 (**Figure 1A**). After genetic characterization, the patient was a compound heterozygote  
242 for two nonsense CTSC mutations (c.96T>G and c401G>A, numbered according to  
243 reference cDNA sequence NM\_001814.4). The first mutation has been previously  
244 described<sup>13</sup> and the second is a novel mutation. Both genetic changes were observed in  
245 the mother and father respectively without phenotypic manifestation, while the brother  
246 did not show any mutation. Patient 2 was a 21-year-old woman with hyperkeratosis in  
247 the palmoplantar region and on her joints and moderate periodontitis (**Figure 1B**). After  
248 genetic characterization, the patient was a compound homozygote for one nonsense  
249 CTSC mutation, c.1286G>A, previously described<sup>14</sup>. This genetic change was observed  
250 in the mother and father in heterozygosis without phenotypic manifestation, while the  
251 brother did not show any mutation. Patient 3 was a XX-year-old woman previously  
252 described (patient L in Table 2, reference 2) with hyperkeratosis in the palmoplantar  
253 region elbows and hands, and suffering from severe periodontitis that led to edentulism.

254 The human CatC sequence is processed into a mature form and it produces a trimer  
255 consisting of the exclusion domain, heavy chain and light chain, which are bound by  
256 disulfide bonds. The active enzyme is composed by a tetramer of these heterotrimers  
257 (**Figure 1D, WT**). Evaluation of the effect of the amino acid changes on the protein  
258 structure of CatC showed the region colored in grey corresponding to the lost sequence  
259 of the one allele. In patient 1, one of the cysteine of the disulfide bond is lost, and it  
260 could affect the 3D structure of the exclusion domain with important consequences on  
261 the function (**Figure 1D, P1**). In patient 2, the amino acids in the active site are all  
262 conserved, not affecting the active site of the enzyme, but probably influencing the  
263 structure, by the folding adopted by the light and heavy chains inducing a possible  
264 effect in the function (**Figure 1D, P2**). In patient 3, only one amino acid in the active  
265 site is conserved with a possible more affected function (**Figure 1D, P3**). Accordingly,  
266 enzymatic activity of CatC was observed reduced in all patients (**Figure 1E**).

### 267 **Fibroblasts from PLS patients show metabolic alterations**

268 Because dermatological symptoms are an important clinical manifestation of PLS, we  
269 evaluated the metabolic status of skin fibroblasts from PLS patients. Fibroblasts from  
270 patients presented a reduced growth ratio and abnormal morphology (**Figure 2A and**  
271 **B**). We also investigated the mitochondrial functionality on fibroblasts from PLS  
272 patients by measuring the OCR values in control and PLS fibroblasts, exposed  
273 sequentially to four modulators of oxidative phosphorylation (OXPHOS): oligomycin  
274 (an inhibitor of  $F_1F_0$ -ATPase or complex V), 2,4-DNP (uncoupling of the OXPHOS  
275 electron transport chain) and antimycin/rotenone (complex I and III inhibitors  
276 respectively) (**Figure 2C**). The basal OCR was markedly affected in fibroblasts from  
277 PLS patients compared to controls (**Figure 2C**). The spare respiratory capacity (SRC)  
278 of cells -an indicator of how close a cell is operating to its bioenergetics limit- was

279 obtained by calculating the mean of OCR values after injection of 2,4-DNP minus the  
280 basal respiration. Fibroblasts from PLS patients showed a significant decrease of SRC  
281 compared to control cells (**Figure 2D**). These metabolic alterations were accompanied  
282 by increased oxidative stress characterized by high levels of reactive oxygen species  
283 (ROS) and mitochondrial superoxide production and reduced activity of the antioxidant  
284 enzymes, superoxide dismutase and catalase (**Figure S1A-D**).

### 285 **Autophagic flux is impaired in PLS**

286 Degradative substrates are cleared intracellularly by a complex macro-autophagic  
287 response <sup>15</sup>. By Western blot and mRNA expression, levels of ATG12 and the  
288 autophagy marker LC3-II were markedly increased in fibroblasts from PLS (**Figure 3A-**  
289 **B**). Furthermore, PLS showed an increment in p62/SQSTM1 accumulation, an  
290 established marker of autophagic clearance (**Figure 3A**). Next, we performed  
291 autophagic flux analysis using the Bafilomycin A1 (BafA1), a specific inhibitor of  
292 vacuolar H<sup>+</sup>-ATPases and a blocker of autophagosome-lysosome fusion, to check for  
293 autophagosome/autophagolysosomal formation. As expected, BafA1 treatment in  
294 control cells led to a significant increase in the amount of LC3-II, suggesting that  
295 autophagic flux is normal (**Figure 3C**). However BafA1 treatment in PLS fibroblasts  
296 had a reduced effect on LC3-II expression levels (**Figure 3C**), indicating that  
297 autophagic flux was impaired (**Figure 3C**). Electron microscopy analysis of fibroblasts  
298 from the patients revealed abundant multilamellar bodies and increased autophagosome  
299 number as indicated by the accumulation of double-membrane vesicle structures  
300 (**Figure 4**).

### 301 **Lysosomal permeability is associated to PLS**

302 Degradation of autophagic substrates/autophagosome takes place in the lysosomal  
303 compartment by acidic proteases, such as cathepsins. Reduced autophagic flux with the  
304 consequent autophagosome accumulation can be a consequence of reduced  
305 autophagosome–lysosome fusion or inefficient lysosomal degradation <sup>16</sup>. According to  
306 this, we determined whether the impaired autophagic flux is associated to lysosomal  
307 dysfunction. Because the cysteine Cats family includes CatB, C, H, K, and L <sup>17</sup>, we  
308 analyzed the level of other important Cat, CatB. Surprisingly, CatB protein levels were  
309 increased in fibroblasts from patients with PLS (**Figure 5A**). Thus, we hypothesized  
310 that lysosomal protease CatB may play an important role in the pathophysiology of PLS  
311 through its release from the lysosomal/autophagolysosomal compartment to the cytosol.  
312 In healthy fibroblasts, CatB signal colocalized with the lysosomal/autophagolysosomal  
313 marker LAMP-1 indicating that it was located within lysosomes/autophagolysosomes  
314 (**Figure 5B**). However, in PLS fibroblasts, the CatB signal was diffuse through the  
315 cytosol and it did not colocalize completely with the LAMP-I marker suggesting  
316 lysosome/autophagolysosome membrane permeabilization (LMP) (**Figure 5B**). This  
317 LMP was also confirmed by the detection of galectin puncta at leaky  
318 autophagolysosomes (**Figure 6**) as it has been described that galectin translocation to  
319 phagosomal and lysosomal membranes is a marker of vacuole lysis and/or  
320 permeabilization <sup>18</sup>. Interestingly, this CatB release and lysosomal alteration were  
321 accompanied by NLRP3-inflammasome activation (**Figure 5C**).

### 322 **Recombinant CatC improves growth and induces partial restoration of autophagic** 323 **flux in fibroblasts**

324 Because mutation in patients induces an important reduction of the enzymatic activity  
325 of CatC, which is associated to an impairment of autophagic flux and lysosomal  
326 dysfunction, we tested the effect of a recombinant CatC (rCatC) in fibroblasts from

327 patients with PLS. First, the rCatC was produced by baculovirus system in insect cell  
328 cultures according to the methods described in Material and methods section <sup>19</sup>. Three  
329 extracts were isolated and tested, supernatant and cellular extracts: insoluble and soluble  
330 extracts. Soluble extract showed more enzyme concentration (tested by Dot Blot) of  
331 rCatC (Figure S2). Immunoblot analysis of the purified rCatC revealed three  
332 polypeptides with molecular masses of approximate 55 kDa, 25 kDa, and 7.8 kDa  
333 (Figure S3). The amount of 55 kDa polypeptides was much larger than that of the other  
334 two. Flatworm CatC expressed in insect cells also exhibited similar three bands of 55  
335 kDa, 25 kDa, and 7.8 kDa polypeptides after purification. Enzymatic activity assay  
336 showed increased enzymatic activity in the soluble extract (Figure S4).

337 After comparing three different doses, rCatC treatment in fibroblasts from a  
338 representative patient showed increased ratio of cell growth in low doses of 0.25 $\mu$ g.  
339 However, control fibroblasts showed an important growth decrement in a dose-  
340 dependent manner (**Figure 7A-C**). Enzymatic activity of CatC was observed to be  
341 partially recovered in the fibroblasts from the patient after 120h of rCatC treatment  
342 (**Figure 7D**). By Western blot analysis, levels of the autophagy marker LC3-II were  
343 markedly increased in fibroblasts from control fibroblasts after rCatC treatment. No  
344 significant changes concerning LC3-II were found in fibroblasts from PLS, taking into  
345 account the increased basal levels of the patient (**Figure 7E**). Furthermore, the increased  
346 level of p62/SQSTM1 accumulation in PLS were recovered by the rCatC treatment after  
347 120h showing an autophagic clearance (**Figure 7E**).

#### 348 **rCatC improves lysosomal permeability associated to PLS**

349 Because we previously showed lysosomal permeability associated to the  
350 pathophysiology of the fibroblasts from PLS, the potential effect of the rCatC on this

351 aspect was also explored. The increased levels of CatB protein previously observed  
352 were decreased in fibroblasts from the patients with PLS after rCatC treatment (**Figure**  
353 **7E**). Thus, partial co-localization of CatB signal with the LAMP-1 marker suggested  
354 a reduction of LMP (**Figure S5**). This reduction of the LMP, was also confirmed after  
355 no detection of galectin puncta at leaky autophagolysosomes (**Figure 8**).

## 356 **Discussion**

357 The dearth of knowledge about the molecular bases of PLS leads to a loss of therapeutic  
358 tools. Previous works have been oriented to the description of new mutations and  
359 several pathophysiological characteristics such as oxidative stress, neutrophilic function  
360 impairment without deepening in molecular mechanisms. The present report provides  
361 experimental evidence about metabolic and autophagic impairment in CatC-deficient  
362 fibroblasts from PLS patients. First, we assessed metabolic changes in cultured  
363 fibroblasts. As expected, a reduction of mitochondrial metabolic rate was observed.  
364 This entailed a significant reduction in cell growth. Then, we provided experimental  
365 evidence for the activation of autophagy in CatC-deficient fibroblasts. From an  
366 ultrastructural and functional point of view, autophagy is characterized by the formation  
367 of double-membraned vesicles called autophagosomes. Autophagic process is initiated  
368 by the formation of a phagophore or nucleation membrane to which cytoplasmic content  
369 is targeted. This phagophore is elongated and results in a new autophagosome which  
370 engulfs material marked for degradation. Finally, mature autophagosomes fuses with  
371 lysosomes, resulting in autophagolysosomes, and the content is degraded via catalytic  
372 enzymes <sup>15</sup>. Enhanced autophagy may be due to either increased autophagosome  
373 formation or impaired clearance of the autophagosomes. Because the autophagosome is  
374 an intermediate structure, the number of autophagosomes observed at any specific time  
375 point is a result of the balance between the rate of their generation and the rate of their

376 conversion into autophagolysosomes. As LC3-II overexpression can evoke either an  
377 increment of autophagy or an impairment of the autophagic flux, these LC3-II changes  
378 must be interpreted together with the p62/SQSTM1 levels <sup>20</sup>. We observed an impaired  
379 autophagic flux determined by expression of LC3-II and increased expression of  
380 proteins involved in clearance pathways like p62/SQSTM1 and confirmed by BafA1  
381 assay and TEM. Interestingly, this blockade of autophagosome fusion with lysosomes  
382 or autophagic flux occurs in multiple lysosomal diseases like Niemann pick, Gaucher  
383 and Pompe diseases <sup>21-23</sup>.

384 Oxidative stress has been associated to the pathophysiology of PLS <sup>2</sup> and we observed  
385 increased ROS production accompanied by reduced antioxidant defenses. Oxidative  
386 stress is associated to the induction of lysosomal instability and membrane  
387 permeabilization <sup>24</sup>. Previously, reduction in some cysteine Cats family members like  
388 CatL have been related to upregulate the CatB and with autophagy dysfunction <sup>25</sup> in a  
389 compensatory transcriptional upregulation with increased enzymatic activation of CatB.  
390 Furthermore, in a lysosomal disease such as Niemann pick disease, the expression of  
391 mature protein forms for both CatB and CatD are upregulated with accumulation of  
392 autophagosomes <sup>26</sup>. Our findings show reduced enzymatic activity of CatC with a  
393 compensatory upregulation of mature CatB proteins leading to a lysosomal  
394 permeabilization. All these disturbances on the machinery of autophagy and lysosome  
395 metabolism could explain several of the clinical phenotype characteristics of PLS.  
396 Autophagy is a process not only involved in the degradation and recycling of  
397 macromolecules including proteins, lipids and carbohydrates, for the synthesis of  
398 essential components and as an energy supply, but also in the innate and adaptive  
399 immunity against microbial invasion <sup>7</sup>. Accordingly, it is not surprising that defects in  
400 the autophagy process have been linked to a wide range of diseases increasing



401 susceptibility to infections <sup>7</sup>. Thus, many patients with PLS show increased  
402 susceptibility to infections and periodontal disease <sup>2</sup>, which probably could be  
403 associated with autophagy dysfunction. Autophagy is also involved in the homeostasis  
404 of the skin, which is the first line of defense against many different insults. So,  
405 autophagy might have a critical role in the development and progression of skin  
406 diseases. However, the exact mechanism by which autophagy dysfunction could be  
407 involved in the development of skin diseases is still unknown. Nevertheless, several  
408 skin diseases like vitiligo, psoriasis, hyperpigmentation or the skin alteration from  
409 systemic lupus erythematosus, have been related autophagy defects <sup>27</sup> which might lead  
410 to inflammatory cytokine production mediated by p62/SQSTM1, as reported for  
411 psoriatic skin <sup>28</sup>. Accordingly, in the present study a similar autophagy dysfunction with  
412 p62/SQSTM1 in PLS was found, which has been associated with increased production  
413 of inflammatory cytokines <sup>29</sup>. Furthermore, the compensatory upregulation of mature  
414 CatB found here was accompanied by a NLRP3-inflammasome activation. NLRP3-  
415 inflammasome complex is a molecular platform which activates innate immune  
416 defenses through the maturation of proinflammatory cytokines (interleukins IL-1 $\beta$  and  
417 IL-18). This complex is activated by a wide variety of danger signals such as potassium  
418 efflux out of the cell, mitochondrial ROS, translocation of NLRP3 to the mitochondria,  
419 cardiolipin, or the release of cathepsins, like CatB, into the cytosol after lysosomal  
420 destabilization <sup>30</sup>. So, inflammatory characteristics of PLS could be explained by  
421 NLRP3-inflammasome activation.

422 Finally, the treatment and management of PLS is poor and is limited to oral approach  
423 and dermatological damage treatment with emollients, salicylic acid and topical  
424 steroids, with toxic effects in many cases <sup>31</sup>. Therefore, it is important to have effective  
425 pharmacological treatments for PLS based on the molecular etiology of the disease.

426 Accordingly, we designed a strategy to correct several pathophysiological markers  
427 shown in this study. Enzyme replacement therapies have been proposed as an  
428 interesting approach in diseases based on lysosomal alterations <sup>32</sup>. Thus, we treated  
429 fibroblasts from PLS patients with a rCatC isolated from insect cells. Autophagy  
430 dysfunction was corrected with a reduction of lysosomal permeabilization and partial  
431 reduction of CatB. All these changes led to an improvement in cellular growth.

432 To the best of our knowledge, this study shows for the first time a new molecular basis  
433 of the PLS and new pharmacological targets. Furthermore, the use of recombinant CatC  
434 presents an interesting therapeutic approach which will need new studies before being  
435 considered as a treatment in humans. New research lines will be needed to establish  
436 putative therapeutic uses of recombinant CatC by oral or topic administration.

437

#### 438 **Acknowledgements**

439 Authors are indebted with Ms Monica Glebocki for extensive editing of the manuscript.  
440 This work has been supported by Proyecto de Investigación de Excelencia de la Junta de  
441 Andalucía CTS113.

#### 442 **Author Disclosure Statement**

443 All the Authors declare that no conflict of interest exists for any of them.

444

445

446

447

448

## 449 References

- 450 1. Roberts H, White P, Dias I, McKaig S, Veeramachaneni R, Thakker N, et al.  
451 Characterization of neutrophil function in Papillon-Lefèvre syndrome. *J Leukoc*  
452 *Biol.* 2016;100:433-44.
- 453 2. Bullón P, Morillo JM, Thakker N, Veeramachaneni R, Quiles JL, Ramírez-  
454 Tortosa MC, et al. Confirmation of oxidative stress and fatty acid disturbances  
455 in two further Papillon-Lefèvre syndrome families with identification of a new  
456 mutation. *J Eur Acad Dermatol Venereol.* 2014;28:1049-56.
- 457 3. Guarino C, Hamon Y, Croix C, Lamort AS, Dallet-Choisy S, Marchand-Adam  
458 S, et al. Prolonged pharmacological inhibition of cathepsin C results in  
459 elimination of neutrophil serine proteases. *Biochem Pharmacol.* 2017;131:52-67.
- 460 4. Roberts H, White P, Dias I, McKaig S, Veeramachaneni R, Thakker N, et al.  
461 Characterization of neutrophil function in Papillon-Lefèvre syndrome. *J Leukoc*  
462 *Biol.* 2016;100:433-44.
- 463 5. Sørensen OE, Clemmensen SN, Dahl SL, Østergaard O, Heegaard NH, Glenthøj  
464 A, et al. Papillon-Lefèvre syndrome patient reveals species-dependent  
465 requirements for neutrophil defenses. *J Clin Invest.* 2014;124:4539-48.
- 466 6. Méthot N, Rubin J, Guay D, Beaulieu C, Ethier D, Reddy TJ, et al. Inhibition of  
467 the activation of multiple serine proteases with a cathepsin C inhibitor requires  
468 sustained exposure to prevent pro-enzyme processing. *J Biol Chem.*  
469 2007;282:20836-46.
- 470 7. Yin Z, Pascual C, Klionsky DJ. Autophagy: machinery and regulation. *Microb*  
471 *Cell.* 2016;3:588-596.
- 472 8. Settembre C, Fraldi A, Rubinsztein DC, Ballabio A. Lysosomal storage diseases  
473 as disorders of autophagy. *Autophagy.* 2008;4:113-4
- 474 9. Hewitt C, McCormick D, Linden G, Turk D, Stern I, Wallace I, et al. The role of  
475 cathepsin C in Papillon-Lefèvre syndrome, prepubertal periodontitis, and  
476 aggressive periodontitis. *Hum Mutat.* 2004;23:222-8.
- 477 10. Aebi H. Catalase in vitro. *Methods Enzymol.* 1984;105:121–126.
- 478 11. Kakkar P, Das B, Viswanathan PN. A modified spectrophotometric assay of  
479 superoxide dismutase. *Indian J Biochem Biophys.* 1984; 21:130–132.
- 480 12. Aits S, Krickler J, Liu B, Ellegaard AM, Hamalisto S, Tvingsholm S, et al.  
481 Sensitive detection of lysosomal membrane permeabilization by lysosomal  
482 galectin puncta assay. *Autophagy.* 2015;11:1408-1424.
- 483 13. Lefèvre C, Blanchet-Bardon C, Jobard F, Bouadjar B, Stalder JF, Cure S, et al.  
484 Novel point mutations, deletions, and polymorphisms in the cathepsin C gene in

- 485 nine families from Europe and North Africa with Papillon-Lefèvre syndrome. *J*  
486 *Invest Dermatol.* 2001;117:1657-61.
- 487 14. Hart PS, Zhang Y, Firatli E, Uygur C, Lotfazar M, Michalec MD, et al.  
488 Identification of cathepsin C mutations in ethnically diverse papillon-Lefèvre  
489 syndrome patients. *J Med Genet.* 2000;37:927-32.
- 490 15. Codogno P. Shining light on autophagy. *Nat Rev Mol Cell Biol.* 2014;15:153.
- 491 16. Mizushima N, Levine B, Cuervo AM, Klionsky DJ. Autophagy fights disease  
492 through cellular self-digestion. *Nature.* 2008;451:1069–1075.
- 493 17. Kaminsky V, Zhivotovsky B. Proteases in autophagy. *Biochim Biophys Acta*  
494 2012;1824:44–50.
- 495 18. Aits S, Krickler J, Liu B, Ellegaard AM, Hamalisto S, Tvingsholm S, et al.  
496 Sensitive detection of lysosomal membrane permeabilization by lysosomal  
497 galectin puncta assay. *Autophagy.* 2015;11:1408–1424.
- 498 19. Qiu GF, Feng HY, Yamano K. Expression and purification of active  
499 recombinant cathepsin C (dipeptidyl aminopeptidase I) of kuruma prawn  
500 *Marsupenaeus japonicus* in insect cells. *J Biomed Biotechnol.*  
501 2009;2009:746289.
- 502 20. Klionsky DJ, Abdelmohsen K, Abe A, Abedin MJ, Abeliovich H, Acevedo  
503 Arozena A, et al. Guidelines for the use and interpretation of assays for  
504 monitoring autophagy (3rd edition), *Autophagy.* 2016;12:1–222.
- 505 21. Guo H, Zhao M, Qiu X, Deis JA, Huang H, Tang QQ, et al. Niemann-Pick type  
506 C2 deficiency impairs autophagy-lysosomal activity, mitochondrial function,  
507 and TLR signaling in adipocytes. *J Lipid Res.* 2016;57:1644-58.
- 508 22. Aflaki E, Moaven N, Borger DK, Lopez G, Westbroek W, Chae JJ, et al.  
509 Lysosomal storage and impaired autophagy lead to inflammasome activation in  
510 Gaucher macrophages. *Aging Cell.* 2016;15:77-88.
- 511 23. Spampinato C, Feeney E, Li L, Cardone M, Lim JA, Annunziata F, et al.  
512 Transcription factor EB (TFEB) is a new therapeutic target for Pompe disease.  
513 *EMBO Mol Med.* 2013;5:691-706.
- 514 24. Boya P, Kroemer G. Lysosomal membrane permeabilization in cell death.  
515 *Oncogene* 2008;27:6434-51.
- 516 25. Mizunoe Y, Sudo Y, Okita N, Hiraoka H, Mikami K, Narahara T, et al.  
517 Involvement of lysosomal dysfunction in autophagosome accumulation and  
518 early pathologies in adipose tissue of obese mice. *Autophagy.* 2017;13:642-653.

- 519 26. Liao G, Yao Y, Liu J, Yu Z, Cheung S, Xie A, et al. Cholesterol accumulation is  
520 associated with lysosomal dysfunction and autophagic stress in *Npc1* <sup>-/-</sup> mouse  
521 brain. *Am J Pathol* 2007;171:962-75.
- 522 27. Yu T, Zuber J, Li J. Targeting autophagy in skin diseases. *J Mol Med (Berl)*.  
523 2015;93:31-8.
- 524 28. Lee HM, Shin DM, Yuk JM, Shi G, Choi DK, Lee SH, et al. Autophagy  
525 negatively regulates keratinocyte inflammatory responses via scaffolding protein  
526 p62/SQSTM1. *J Immunol*. 2011;186:1248–1258.
- 527 29. Sadik CD, Noack B, Schacher B, Pfeilschifter J, Mühl H, Eickholz P. Cytokine  
528 production by leukocytes of Papillon-Lefèvre syndrome patients in whole blood  
529 cultures. *Clin Oral Investig*. 2012;16:591-7.
- 530 30. Guo H, Callaway JB, Ting JP. Inflammasomes: mechanism of action, role in  
531 disease, and therapeutics. *Nat Med*. 2015;21:677-87.
- 532 31. Sreeramulu B, Shyam ND, Ajay P, Suman P. Papillon-Lefèvre syndrome:  
533 clinical presentation and management options. *Clin Cosmet Investig Dent*.  
534 2015;7:75-81.
- 535 32. Wyatt K, Henley W, Anderson L, Anderson R, Nikolaou V, Stein K, et al. The  
536 effectiveness and cost-effectiveness of enzyme and substrate replacement  
537 therapies: a longitudinal cohort study of people with lysosomal storage  
538 disorders. *Health Technol Assess*. 2012;16:1-543.
- 539
- 540
- 541
- 542
- 543

544 **Figure legends**

545 **Figure 1. A-C.** Pedigree analysis and clinical characteristic of the patients. Black or  
546 gray symbols denote people with different mutations. Symbols with two colors denote  
547 two heteroplasmic mutations. Squares: man, circles: woman. **D.** 3D-structure of a  
548 cathepsin C monomer. The protein is processed into a proteolytically mature active  
549 enzyme consisting of 3 chains: an exclusion domain (flesh color), a heavy chain (green  
550 color) and a light chain (violet color). WT: Canonical structure highlighting a disulfid  
551 bond keeping the folding of the exclusion domain, and the three amino acids of the  
552 active site (pink color). P1: Patient 1. The sort sequence colored in orange corresponds  
553 to one allele, and the region colored in grey corresponds to the lost sequence of the  
554 other allele. Note that one of the cysteines of the disulfide bond is lost, and it could  
555 affect the 3D structure of the exclusion domain. P2: Patient 2. The region colored in  
556 grey corresponds to the lost sequence in the mutant. Note that the amino acids in the  
557 active site are all conserved. P3: Patient 3. The region colored in grey corresponds to the  
558 lost sequence in the mutant. Note that only one amino acid in the active site is  
559 conserved. **E.** Enzymatic activity of CatC in homogenate from skin fibroblasts. Data  
560 represent the mean – SD of three separate experiments. \*\*\* $p < 0.001$  between controls  
561 and PLS patients.

562 **Figure 2.-** Abnormalities in various aspects of bioenergetic function. **A.** Morphological  
563 changes of fibroblasts from patients compared with control. **B.** Cell growth determined  
564 in healthy and PLS fibroblasts. **C.** Oxygen consumption rate (OCR) in cells from  
565 control and PLS patients. OCR was monitored using the Seahorse XF-24 Extracellular  
566 Flux Analyzer with the sequential injection of oligomycin (2.5 $\mu$ g/mL), 2,4-DNP  
567 (1mM), antimycin (10 $\mu$ M)/rotenone (1 $\mu$ M) at the indicated time point. **D.** The spare  
568 respiratory capacity (SRC) of FM fibroblasts showed a significant decrease compared to

569 control fibroblasts. Data represent the mean $\pm$ SD of three separate experiments. \* $P <$   
570  $0.05$ ; \*\* $P < 0.01$ ; \*\*\* $P < 0.001$  between control and PLS patients.

571 **Figure 3.- A.** Autophagic protein expression levels of ATG12, LC3-I (top panels, top  
572 band), LC3-II (top panels, bottom band), and p62 were determined in control and PLS  
573 fibroblast cultures by Western blot analysis, as described in Materials and Methods.  
574 ATG12 band represents the Atg12-Atg5 conjugated form. GAPDH was used as a  
575 loading control. **B.** Impaired autophagic flux in PLS fibroblasts. Determination of LC3-  
576 II in the presence and absence of bafilomycin A1 in control (CTL) and PLS fibroblasts  
577 (patients). Control and PLS fibroblasts were incubated with bafilomycin A1 (100 nM  
578 for 12 h). Total cellular extracts were analyzed by immunoblotting with antibodies  
579 against LC3. GAPDH was used as a loading control. For control cells, data are for  
580 experiments on 2 different control cell lines.

581 **Figure 4.- Ultrastructure of PLS fibroblasts. A.** Control fibroblasts showing  
582 mitochondria with typical ultrastructure. **B.** Lamellar bodies (black arrows) and  
583 autophagosome (white arrows) present in PLS fibroblasts. Scale bar 10  $\mu$ m (low  
584 magnification) and 2  $\mu$ m (high magnification).

585 **Figure 5.- Cathepsin B releases in PLS fibroblasts. A.** Protein expression levels of  
586 CatB B were determined in control and PLS fibroblast cultures by Western blotting, as  
587 described in Materials and Methods. **B.** Immunofluorescence of CatB in control and  
588 pathological cells. Note that in PLS fibroblasts CatB diffuses throughout the cytosol. **C.**  
589 NLRP3-inflammasome protein expression levels of NLRP3 (top band) and Caspase 1  
590 (intermediate bands), were determined in control and PLS fibroblast cultures by  
591 Western blot analysis, as described in Materials and Methods. GAPDH was used as a  
592 loading control.



593 **Figure 6.-** Representative fluorescence images of fibroblasts from control and PLS.  
594 Cells were fixed and stained with anti-Galectin-3 antibodies (green) and anti-LAMP-I  
595 (red). Nuclei were stained with Hoechst 33342 (blue). Increased Galectin-3- puncta and  
596 colocalization of Galectin-3 and LAMP-I puncta are shown in patients.

597 **Figure 7.- A-C.** Cell growth with rCatC determined in healthy and representative PLS  
598 fibroblasts. **D.** Enzymatic activity of CatC in homogenate from skin fibroblasts after  
599 120h of rCatC treatment. Data represent the mean – SD of three separate experiments.  
600 \* $p < 0.01$  between controls and control treated with rCatC; <sup>a</sup> $p < 0.01$  between PLS and  
601 PLS treated with rCatC. **E.** Autophagic protein expression levels of LC3 and p62, CatB  
602 were determined in control and representative PLS fibroblast cultures after rCatC  
603 treatment by Western blot analysis, as described in Materials and Methods. GAPDH  
604 was used as a loading control. For control cells, data are for experiments on 2 different  
605 control cell lines.

606 **Figure 8.-** Representative fluorescence images of fibroblasts from control and PLS to  
607 evaluate the effect of the rCatC in lysosomal permeabilization. Cells were fixed and  
608 stained with anti-Galectin-3 antibodies (green) and anti-LAMP-I (red). Nuclei were  
609 stained with Hoechst 33342 (blue). Increased Galectin-3- puncta and colocalization of  
610 Galectin-3 and LAMP-I puncta are shown in patients.

611

612

613

614

615

## SUPPLEMENTARY DATA

616

617 **Autophagic dysfunction in Papillon Lefèvre is restored by recombinant Cathepsin**  
618 **C treatment**

619 Pedro Bullón<sup>1,2\*</sup>, Beatriz Castejón-Vega<sup>1\*</sup>, Lourdes Román-Malo<sup>1</sup>, María Paz Jiménez-  
620 Guerrero<sup>3</sup>, David Cotán<sup>3</sup>, Tamara Y. Forbes-Hernandez<sup>4</sup>, Alfonso Varela-López<sup>5</sup>,  
621 Antonio Pérez-Pulido<sup>6</sup>, Francesca Giampieri<sup>4</sup>, José L. Quiles<sup>5</sup>, Maurizio Battino<sup>4</sup>, José  
622 A. Sánchez-Alcázar<sup>3</sup>, Mario D. Cordero<sup>5</sup>

623 <sup>1</sup> Research Laboratory, Dental School, University of Sevilla, Sevilla, Spain

624 <sup>2</sup> Dept. of Periodontology, Dental School, University of Sevilla, Spain.

625 <sup>4</sup> Dipartimento di Scienze Cliniche Specialistiche ed Odontostomatologiche, Sez.  
626 Biochimica, Università Politecnica delle Marche, Ancona, Italy.

627 <sup>5</sup> Department of Physiology, Institute of Nutrition and Food Technology "José Mataix",  
628 Biomedical Research Center (CIBM), University of Granada, Armilla, Avda. del  
629 Conocimiento s.n., 18100 Armilla, Spain.

630 <sup>6</sup> Centro Andaluz de Biología del Desarrollo (CABD), Universidad Pablo de Olavide-  
631 CSIC-Junta de Andalucía.

632 \* These authors contributed equally to this work.

633 **Running Title:** Autophagic dysfunction in Papillon Lefèvre

634

635 **Corresponding Author:**

636 Dr. Mario D. Cordero  
637 Institute of Nutrition and Food Technology "José Mataix Verdú", Department of  
638 Physiology, Biomedical Research Center, University of Granada, 18100 Granada,  
639 Spain. +34-958-241-000 (ext. 20316), Email: [mdcormor@ugr.es](mailto:mdcormor@ugr.es)

640

641

642

643

644

645

646

647

648

649

650

651

652

653

654

655

656

657

658

659

660

661

662

663

664

665

666

667

668

669

670

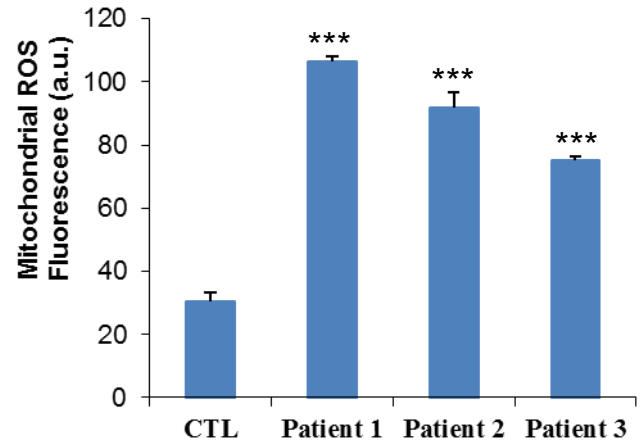
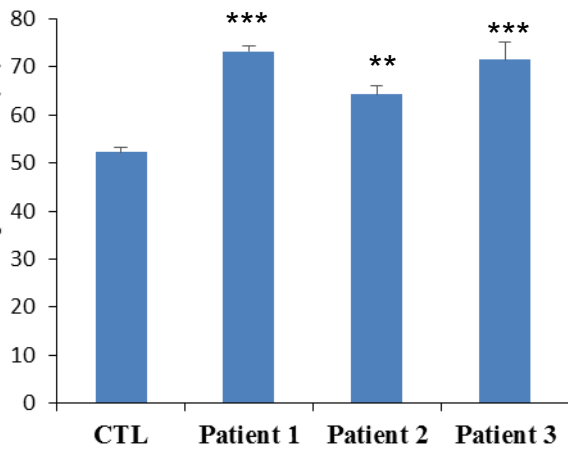
671

672

673

674

675



655

656

657

658

659

660

661

662

663

664

665

666

667

668

669

670

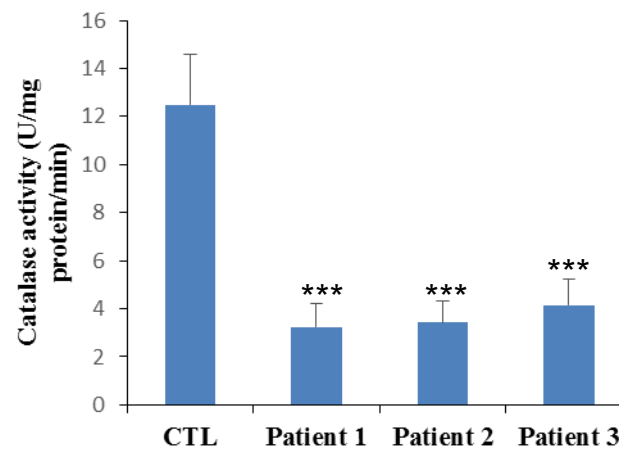
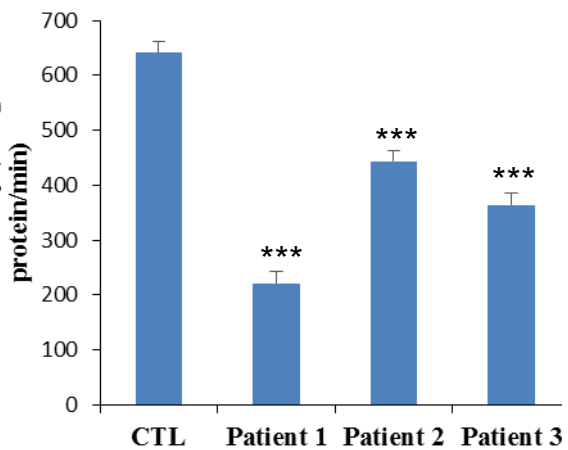
671

672

673

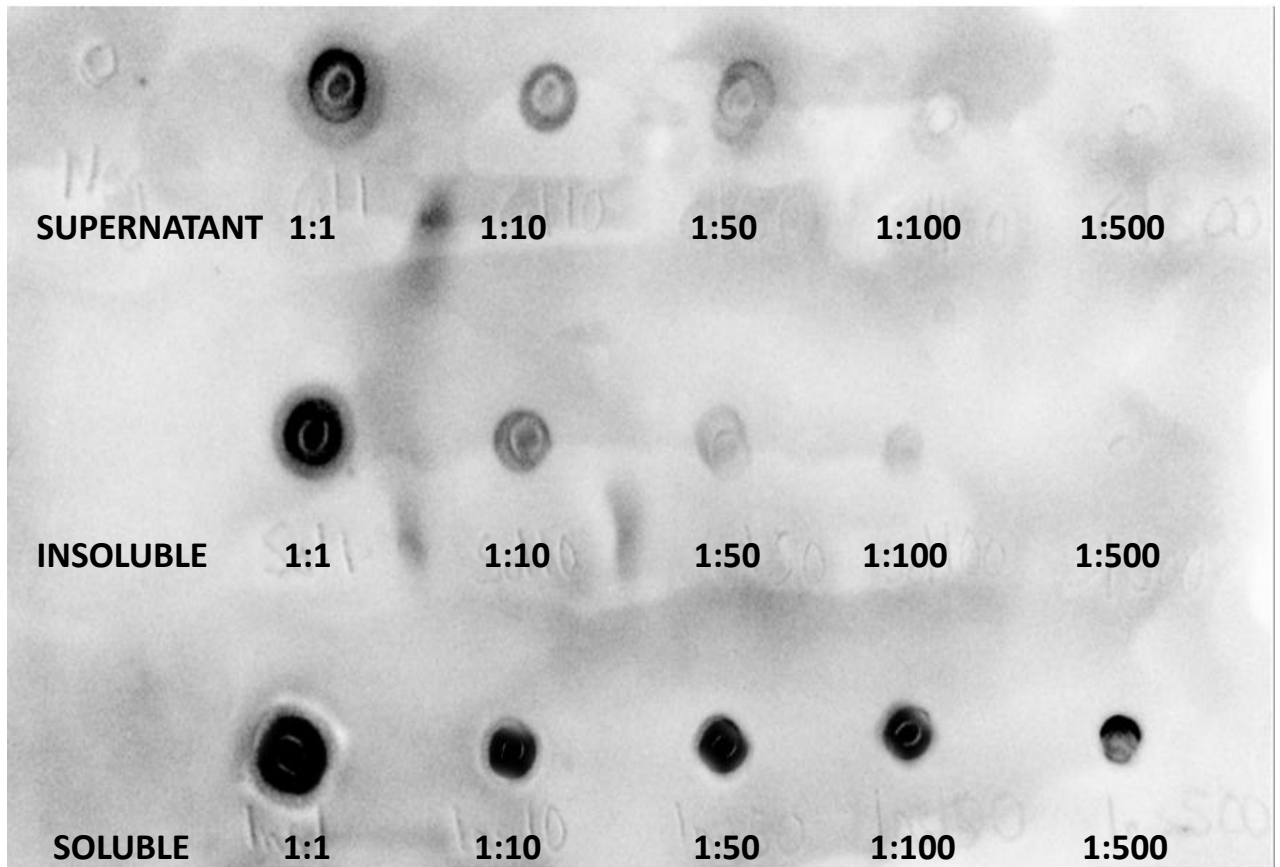
674

675



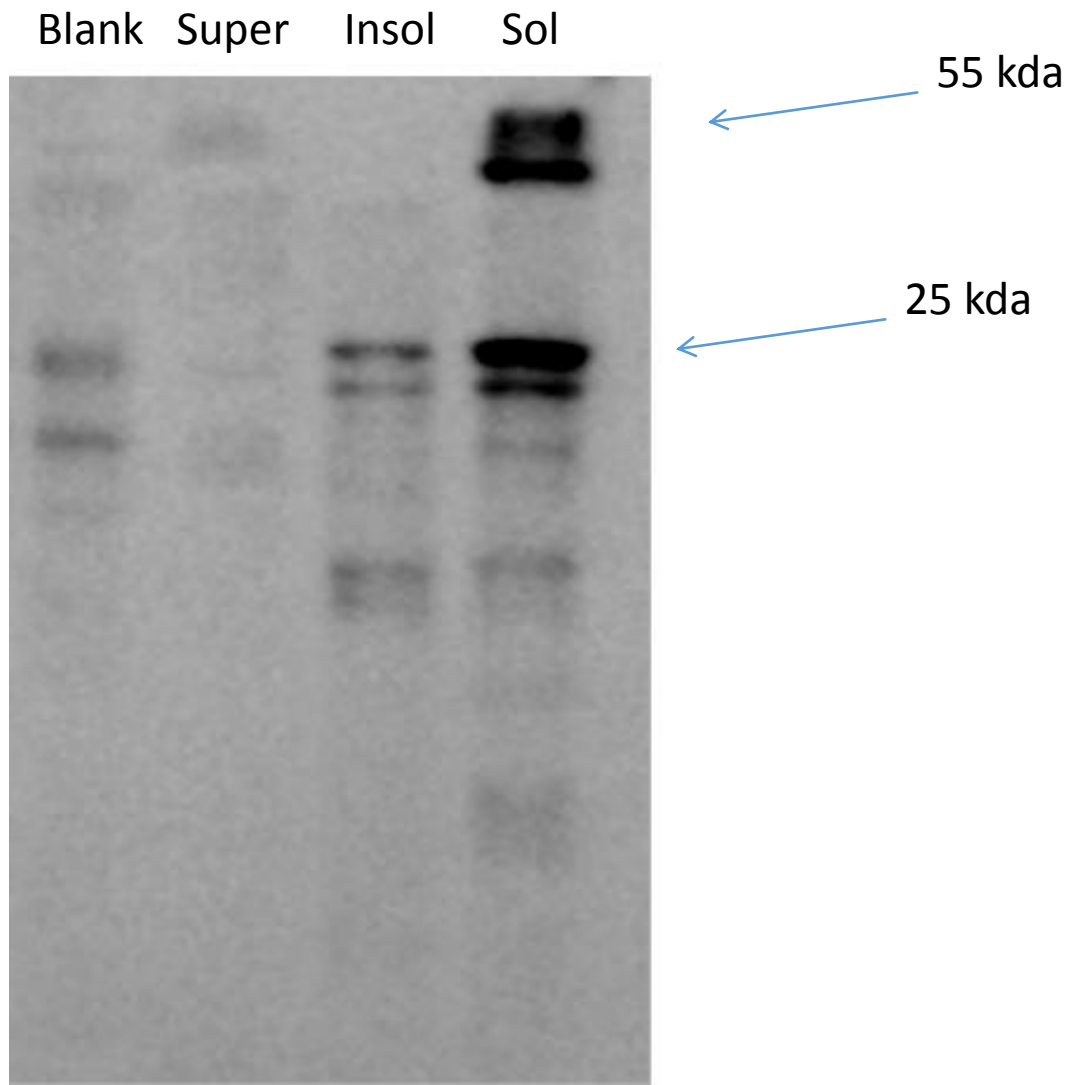
**Supplementary figure 1.** Oxidative stress and oxidative damage levels in fibroblasts from PLS patients. (A and B) Total ROS and mitochondrial ROS production were analyzed in fibroblasts from control and PLS patients by flow cytometry as described in Material and Methods. (C and D) Antioxidant enzymes SOD and catalase (CAT) activities were also analyzed in fibroblasts from control and PLS patients as described in Material and Methods. Data represent the mean±SD of three separate experiments.\*P < 0.05, \*\*P < 0.01 and \*\*\*P < 0.001 between control and PLS patients.

674  
675  
676  
677  
678  
679  
680  
681  
682  
683  
684  
685  
686  
687  
688  
689  
690  
691  
692  
693  
694  
695  
696  
697  
698  
699  
700  
701



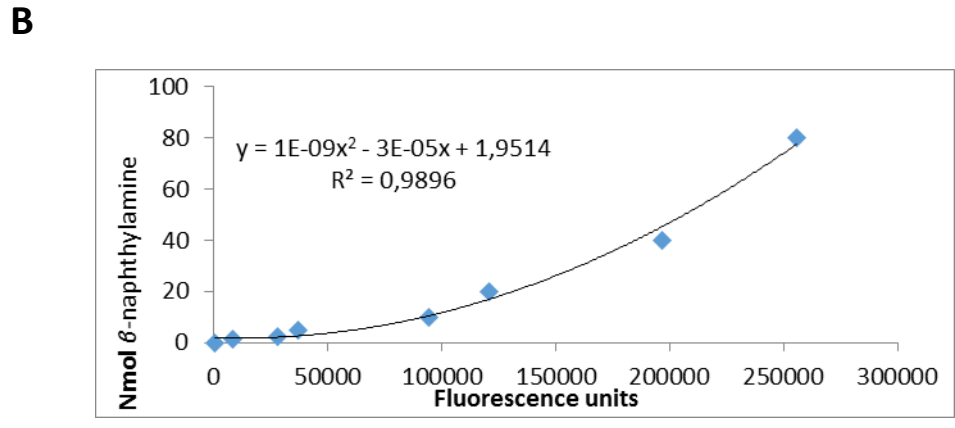
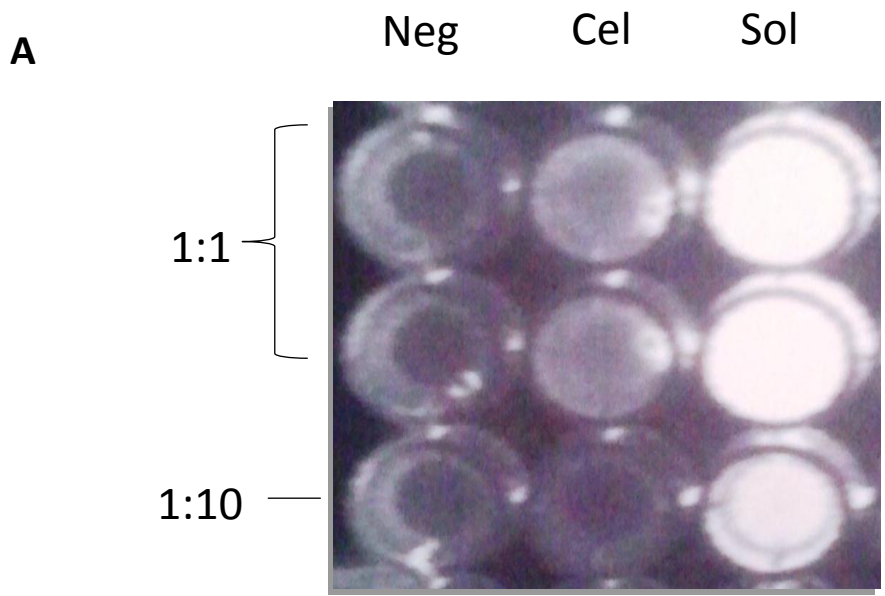
**Supplementary figure 2.** Detection of CatC protein in theof three different extracts (cell extract and the soluble and insoluble extract) determined by Dot Blot.

702  
703  
704  
705  
706  
707  
708  
709  
710  
711  
712  
713  
714  
715  
716  
717  
718  
719  
720  
721  
722  
723  
724  
725  
726  
727  
728  
729



**Supplementary figure 3.** Immunoblot analysis of the insoluble extract revealed three polypeptides with molecular masses of approximate 55 kDa, 25 kDa, and 7.8 kDa. Super: supernatant, Insol: insoluble, Sol: soluble.

730  
731  
732  
733  
734  
735  
736  
737  
738  
739  
740  
741  
742  
743  
744  
745  
746  
747  
748  
749  
750  
751  
752  
753  
754  
755  
756

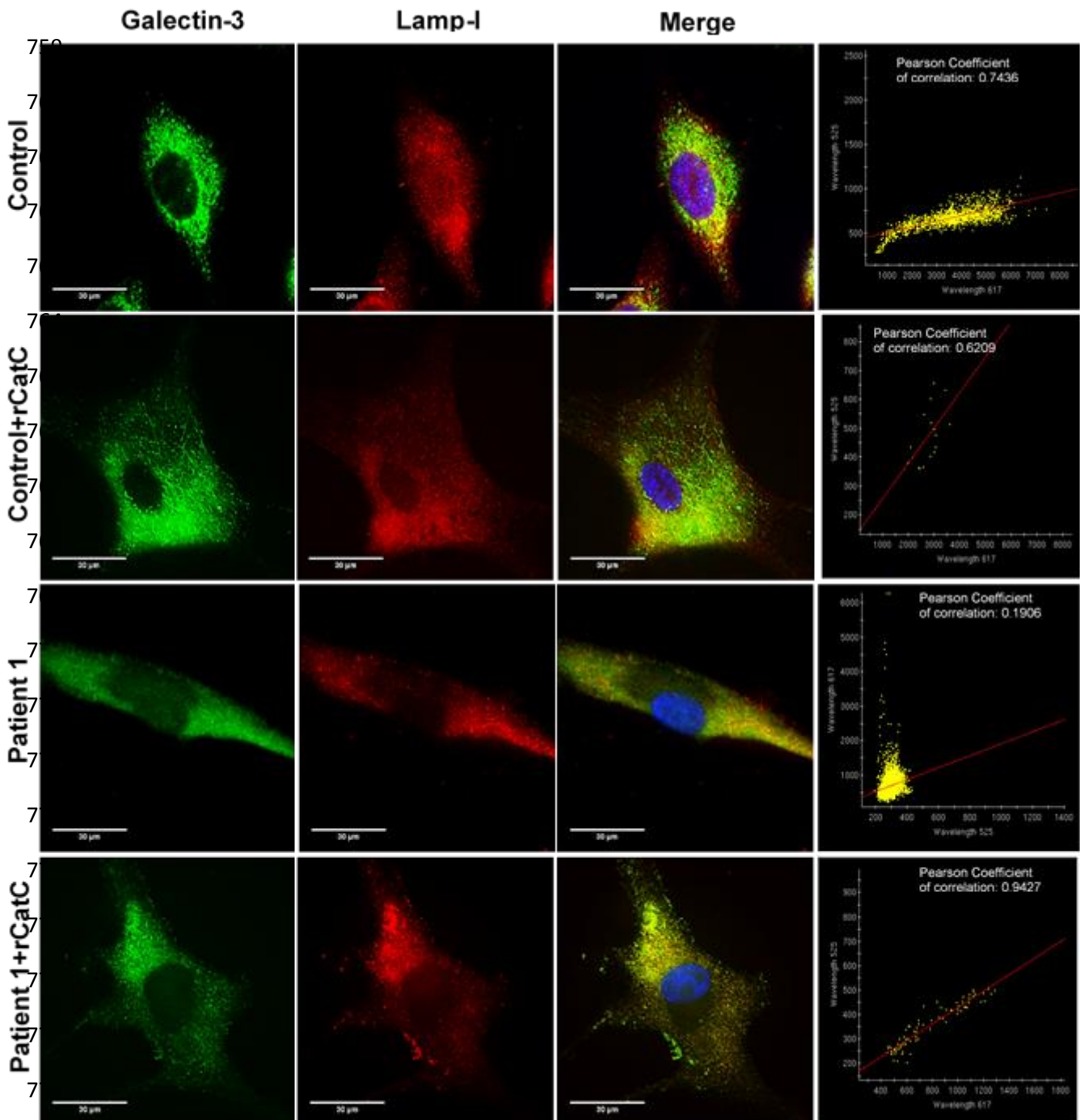


	Negative	Cell	Soluble
Mean	17810	50023,5	186078,5
SD	6940	9337	82154

**Supplementary figure 4.** Enzymatic activity of cellular and soluble extracts.

757

758



779

780 **Supplementary figure 5.** Representative fluorescence images of fibroblasts from  
 781 control and PLS with and without rCatC. Cells were fixed and stained with anti-  
 782 Galectin-3 antibodies (green) and anti-LAMP-I (red). Nuclei were stained with Hoechst  
 783 33342 (blue). Increased Galectin-3- puncta and colocalization of Galectin-3 and LAMP-  
 784 I puncta are shown in patients.

785

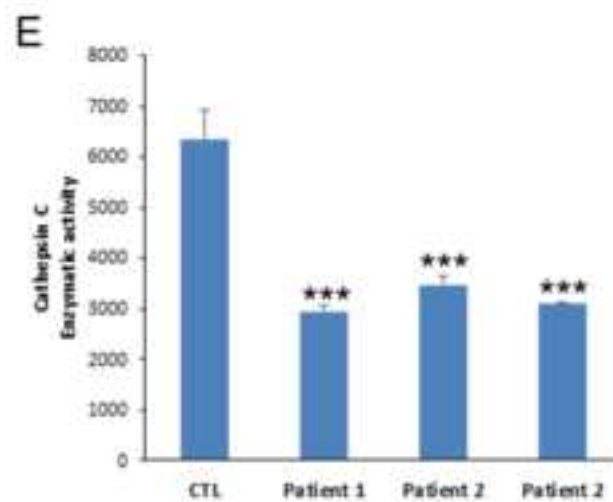
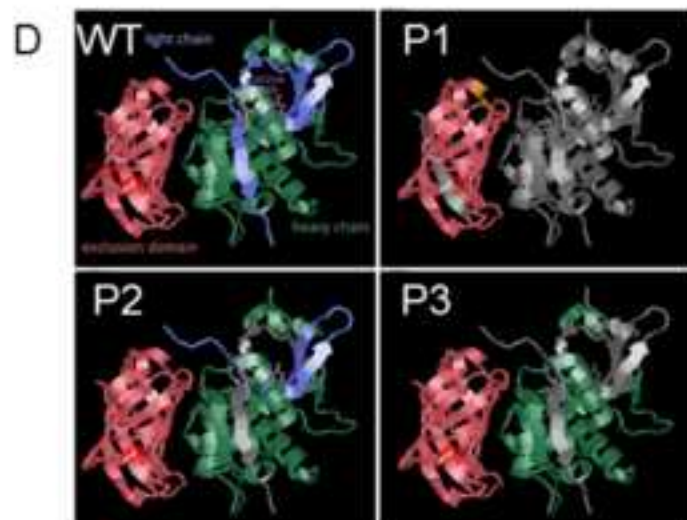
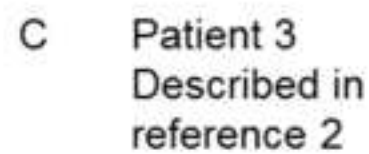
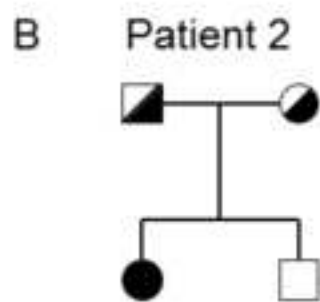
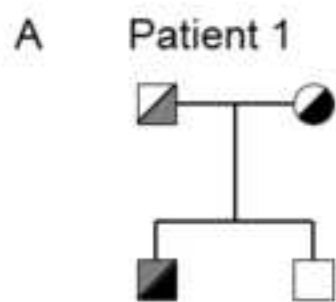
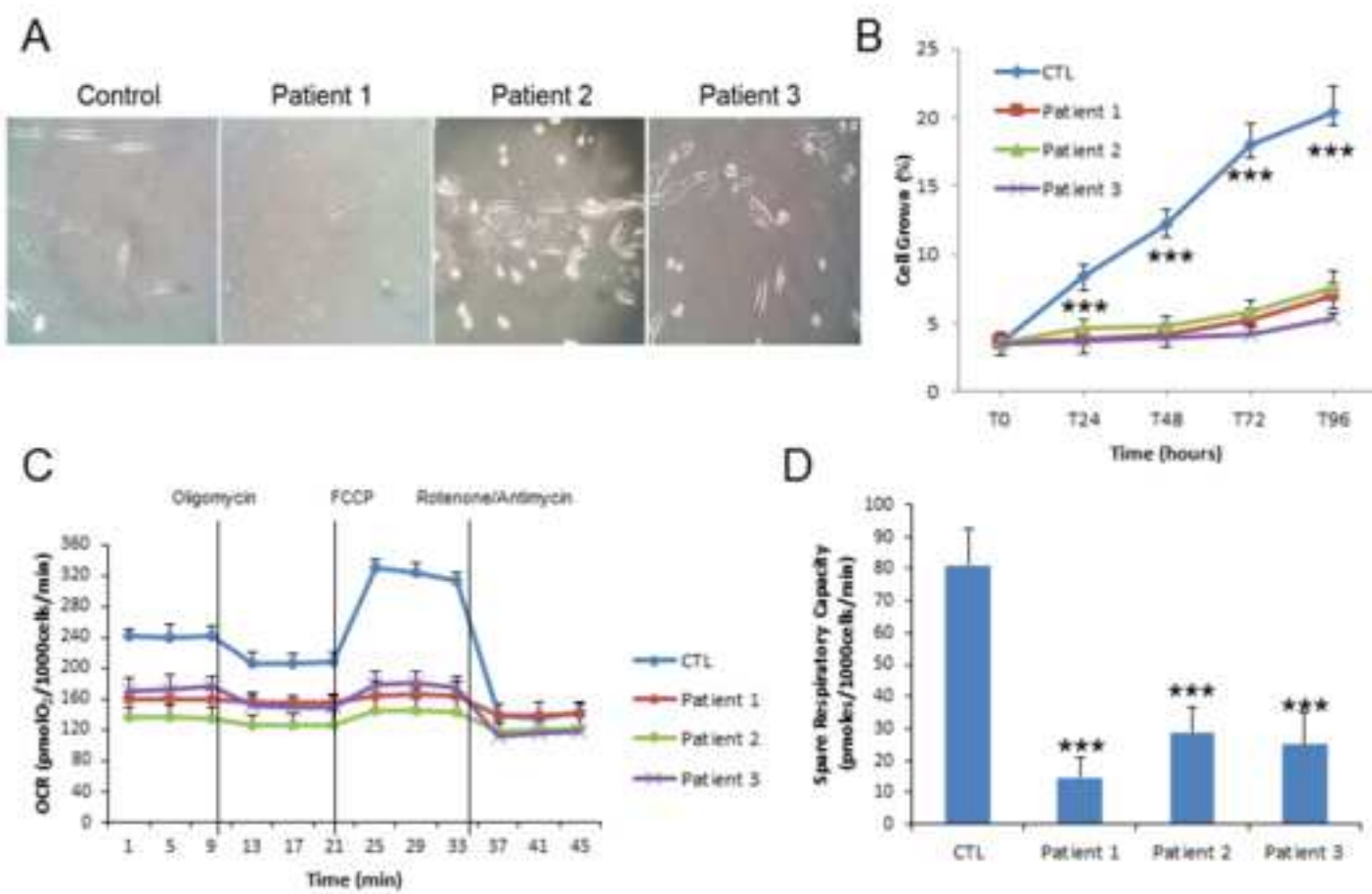
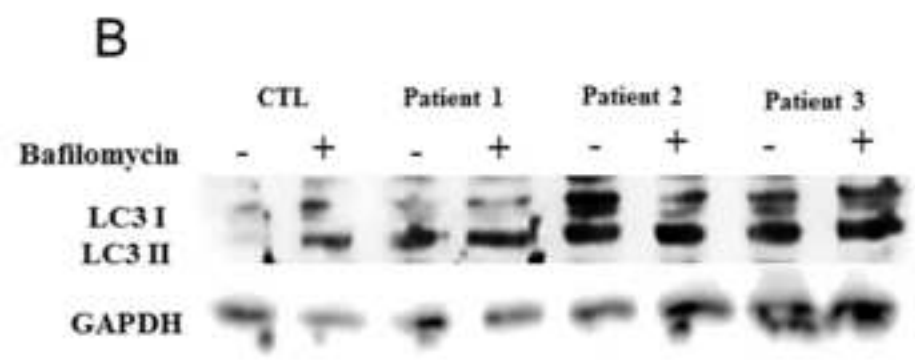
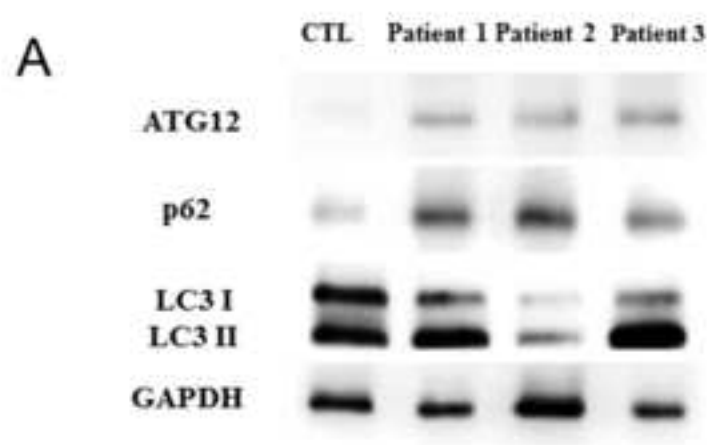
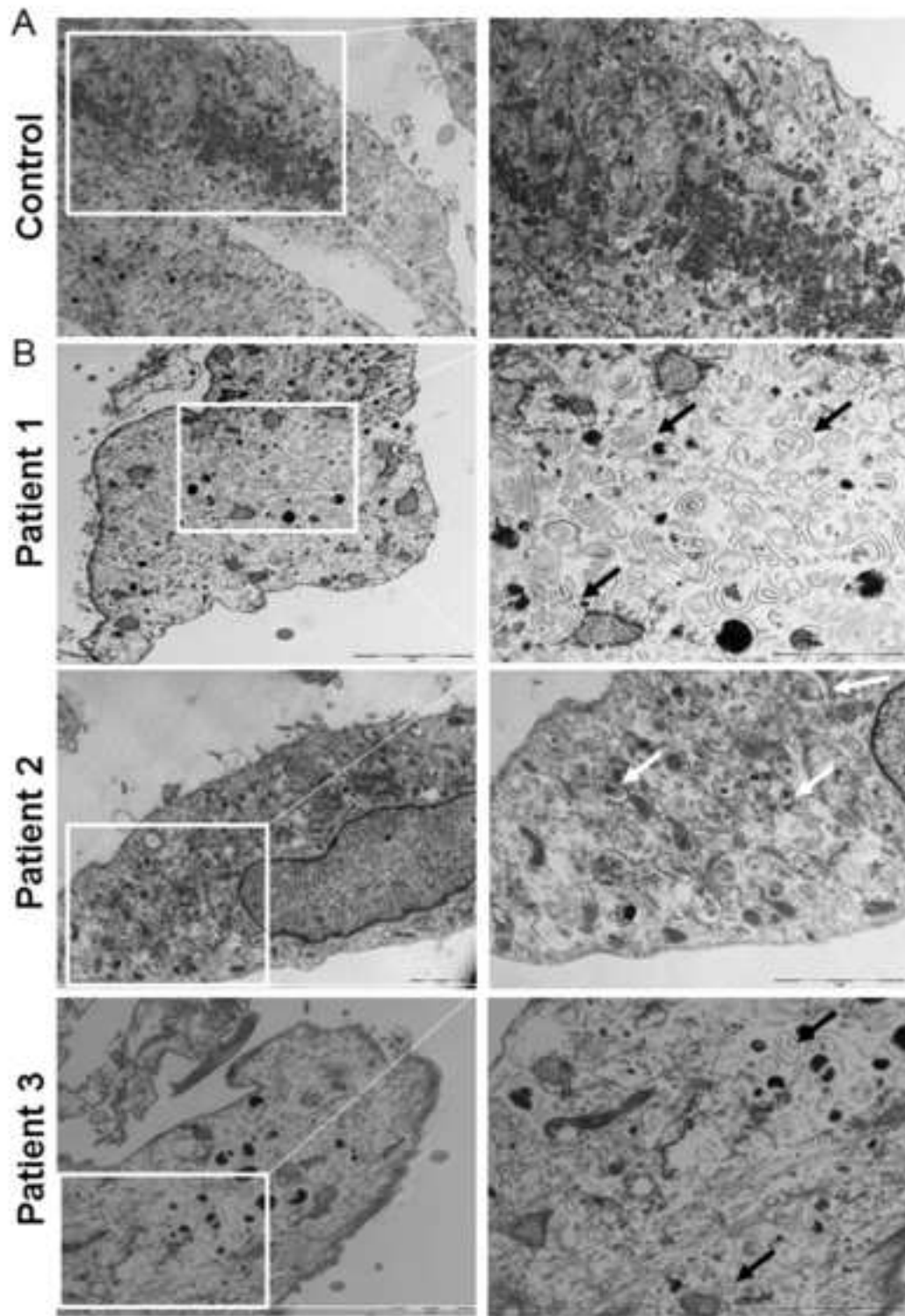




Figure No.  
[Click here to download high resolution image](#)







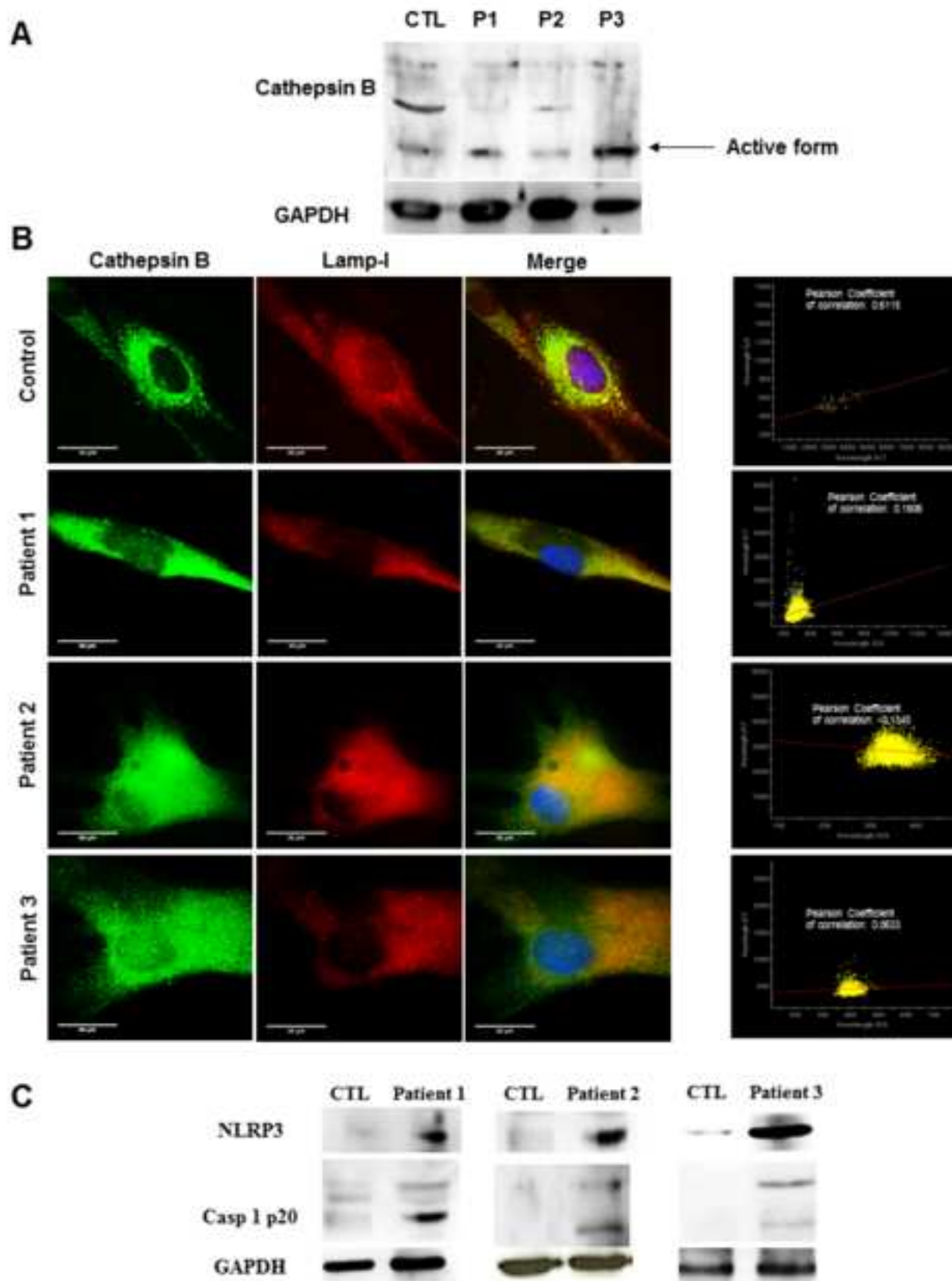


Figure No. [Click here to download high resolution image](#)

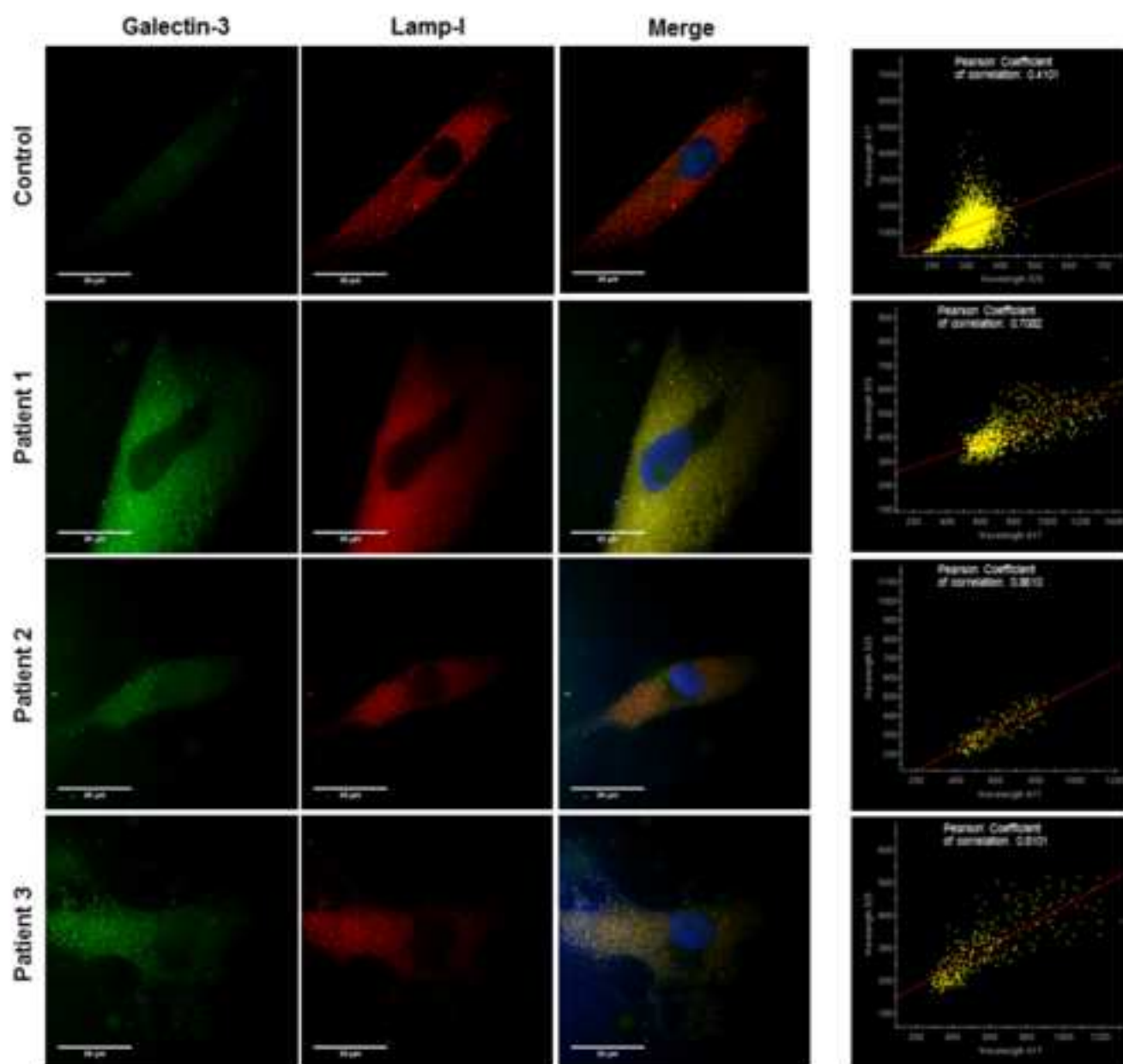


Figure No.  
[Click here to download high resolution image](#)

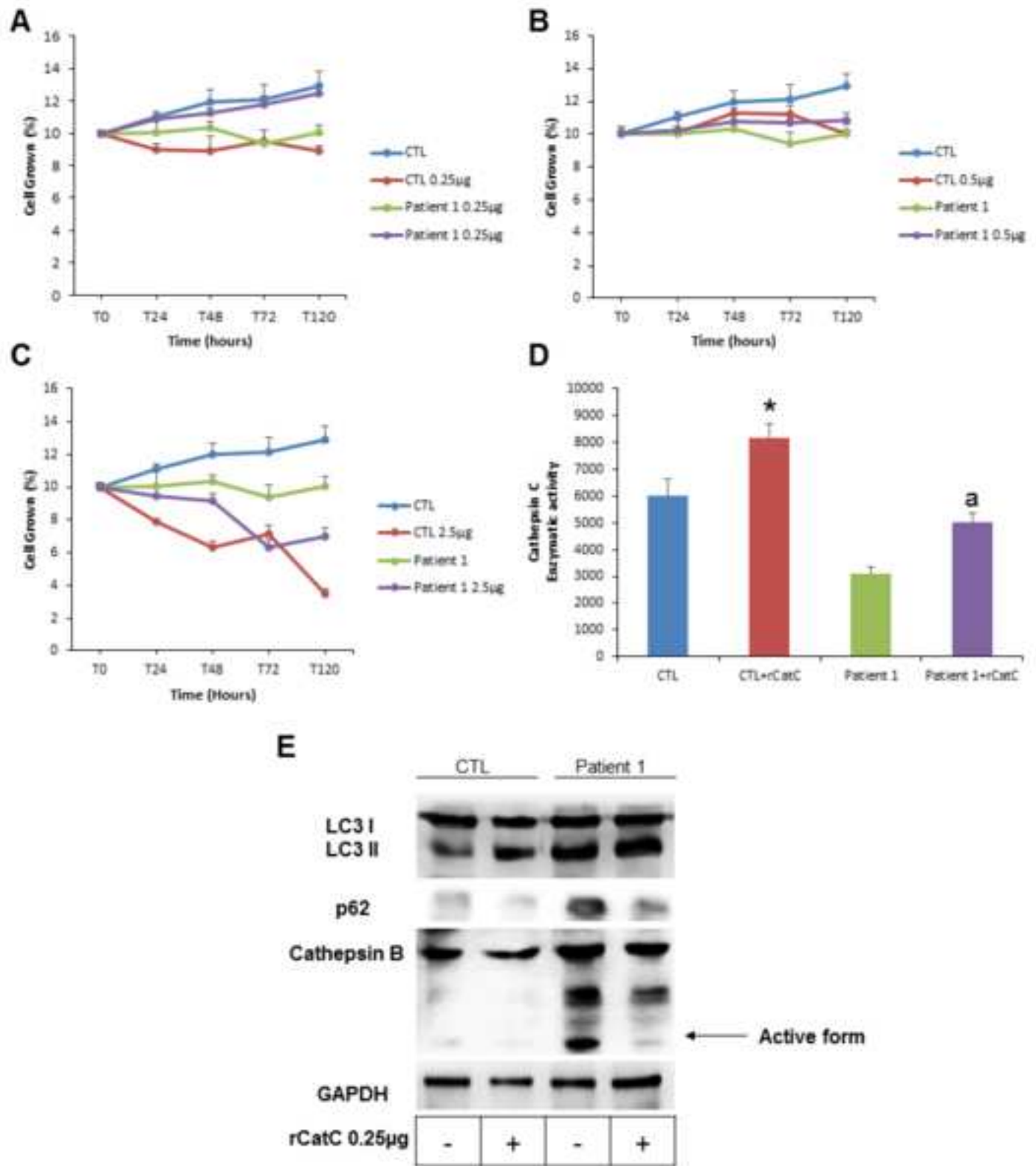


Figure No. [Click here to download high resolution image](#)

